12-2021

Shear Strength of Concrete Beams made with Belitic Calcium Sulfoaluminate Cement

Caleb W. Chesnut
University of Arkansas, Fayetteville

Shear Strength of Concrete Beams made with Belitic Calcium Sulfoaluminate Cement

A thesis submitted in partial fulfillment
of the requirements for the degree of
Master of Science in Civil Engineering

by

Caleb W. Chesnut
University of Arkansas
Bachelor of Science in Civil Engineering, 2020

December 2021
University of Arkansas

This thesis is approved for recommendation to the Graduate Council.

_____
Cameron Murray, Ph.D.
Thesis Advisor

_____
Micah Hale, Ph.D.
Committee Member

_____
Eric Fernstrom, Ph.D.
Committee Member

Abstract

The need for a cleaner alternative to portland cement (PC) concrete has led to increasing interest in alternatives to PC. Structural properties of most of these alternative cements are still an open research topic. One promising alternative cement is belitic calcium sulfoaluminate (BCSA) cement. The study presented in this paper investigated the shear strength, long term compressive strength, and carbonation in BCSA cement and PC concrete beams. A total of twelve eight-foot long beams were made; eight BCSA cement concrete beams and four PC concrete beams to be tested at various ages depending on cement type. Two beams of each cement type were tested in shear at each age. The BCSA cement concrete beams were tested at three hours, one day, twenty-eight days, and one year. The PC concrete beams were tested at twenty-eight days and one year. The four one-year beams were stored outside until they were tested, and the remaining eight beams were stored in a lab environment. Cross-sections were cut out of the one-year beams and the pH was tested to determine carbonation depths. Three cylindrical cores were cut out of each one-year beam and a compressive strength test was performed per ASTM C24 [1]. BCSA cement concrete beams behaved similarly and had similar shear strength when compared to PC concrete beams. Code estimated shear strengths of BCSA cement concrete beams were more conservative than those for PC concrete beams. No visible carbonation was detected in either BCSA cement concrete or PC concrete beams. Compressive strengths of the cores showed increased strengths over time in BCSA cement concrete, similar to PC concrete.

Acknowledgements

The completion of this thesis and research project would not have been possible without help from many people and organizations.

First, I want to thank God for leading me to where I am. One can say it was luck or a blessing that I fell into the Civil Engineering department at the University of Arkansas and was able to succeed. I tend to lean towards the latter.

I would like to thank CTS Cement for the generous donation of the BCSA cement used in this study and providing monetary support.

I also want to thank my parents Mark and Donna Chesnut for their continued support throughout the entirety of my education. Their constant encouragement to be better, do better, and to chase my dreams is something I will cherish for my entire life.

A big thank you goes out to my old lab partner Gerardo Aguilar for his help with my first taste of research while completing my undergraduate honors thesis. I learned a lot from him that I was able to implement in this most recent project. And also, to my current lab partners and friends: Rilye Dillard, Bette Poblete, and most importantly Wes Keys and Behzad Farivar. I could not have accomplished the amount that I did in such a short time without help from those listed before. From early mornings at the old Panty Hose Factory lab (otherwise known as the University of Arkansas Engineering and Research Center) to working into the evening at the brand new Grady E. Harvell Civil Engineering Research and Education Center (CEREC).

Another “thank you” goes out to the Arkansas Academy of Civil Engineering for not only awarding me a scholarship during my time at the University of Arkansas but for their generous support towards the building of the Grady E. Harvell CEREC. And to Mr. Grady Harvell for the

years of effort that he put into making CEREC a reality. The new lab truly has changed how and what we are able to do research wise.

I am forever grateful for Dr. Cameron Murray taking me into his lab group during my undergraduate degree. The amount I have learned and the skills that I have developed from that time on will be forever valuable. I also want to thank my Calculus I with Review professor, Dr. Shanda Hood. She may not know it, but her belief in me during the first semester, after I took a wild leap from Business to Engineering, was a huge contributing factor to my persistence in the program and ultimately my success.

Lastly, I give a special thanks to my beautiful wife. Your support for the past eight years means more to me than you will ever know. From me being a low aspiring “just enough to get by” high school student to a fledgling structural engineer, you have been through it all. Thank you.

Epigraph

"In general, the problems of Civil Engineers
are given to them by God Almighty.
They are the problems of nature."
Hardy Cross, Engineers and Ivory Towers 1952

1. Introduction

Due to the rising concern about global climate change, engineers and the construction industry are trying to mitigate the impacts of concrete construction. One area for improvement is the implementation of environment friendly alternative cementitious materials to portland cement (PC) such as belitic calcium sulfoaluminate cement (BCSA). BCSA cement is not only better for the environment, but it, unlike some other alternative cementitious materials, is mixed in the same way that PC concrete is. This allows for easier industry adoption compared to alkali activated cements, magnesium phosphate cements, or other chemically activated alternative binders.

In ACI 318-19, there is a new allowance for design engineers to specify alternative cement types for use in structural concrete as long as they can prove that the material meets or exceeds the properties of PC concrete [2]. Before this can, happen much needs to be known about the fresh and hardened properties of BCSA cement concrete. Past research has been completed on set retarder effectiveness, mix design, and flexural strength of BCSA cement concrete [3-6]. This project aims to build on past research and evaluate the shear strength of BCSA cement concrete beams while also investigating the long-term carbonation and compressive strength of BCSA cement concrete.

In this study, eight BCSA cement concrete beams and four PC concrete beams with no transverse reinforcement were made and tested to evaluate their shear strength at different ages. Additionally, two BCSA cement concrete and two PC concrete beams were cut open after more than a year stored outdoors to determine the depth of carbonation, and three cores from each of those beams were tested to measure the long-term compressive strength. The experimental shear values were compared to shear capacity equations from the American Concrete Institute (ACI)

318-14 & 318-19 Building Codes for Structural Concrete, the American Association of State Highway and Transportation Officials (AASHTO) Load and Resistance Factor Design (LRFD) Bridge Design Specifications (2017), Eurocode 2: Design of Concrete Structures (1992), and the Simplified Modified Compression Field Theory (SMCFT) [7-11].

2. Background

2.1 Belitic calcium sulfoaluminate cement

BCSA cement is a fast-setting, high-early strength alternative to PC. Calcium sulfoaluminate (CSA) cement, also known as Klein's compound or Ye'elimite, was first developed in the United States in the 1950s and 1960s by Dr. Alexander Klein at UC Berkeley. Later, cement formulations including CSA and belite were developed to reduce the naturally expansive properties of CSA [12], the first of which was patented by Ost, Schiefelbein, and Summerfield in 1975 [13]. Due to its rapid setting time and early-age strength gain, BCSA has been primarily used for repairs of bridges, roadways, and runways [14]. Little is known about the performance and behavior of BCSA when used as structural concrete due to its limited use in structural applications. Potential uses for BCSA cement include precast pretensioned concrete [15], accelerated bridge construction (ABC), emergency repairs [14], and thermal energy storage [16].

The production of BCSA cement results in reduced environmental impacts when compared to PC. Production of cement contributed 5-7% of global carbon dioxide (CO_2) emissions in 2009, mostly from the production of PC [17]. During the production of PC, a mixture of limestone and clay is heated at 1500°C to produce PC clinker. CO_2 is emitted from the decomposition of limestone and the energy input required to reach the high kiln temperatures [18]. BCSA cement clinker requires less limestone in the raw materials and forms at a lower

temperature (1250°C) than PC, so it requires less energy to produce. The combined effect is a reduction in carbon emissions of about 30-50% compared to PC [19]. The largest drawback for BCSA cement is its cost. According to Thomas et al. [19], BCSA cement costs as much as four times more than Type I/II PC. This is partly due to economies of scale associated with PC production and could change with increased demand leading to increased production. However, an alumina source is required to produce BCSA cement, and there are few sources of alumina in the United States [20].

Past research has largely focused on material properties of BCSA cement and less on the performance and behavior of structural concrete members made with BCSA cement [2, 21]. Studies such as Bowser et al. 2020 [15] have investigated structural properties of precast concrete members made with BCSA cement concrete. In addition, Cook et al. [22], investigated the flexural strength and behavior of reinforced BCSA cement concrete beams. Research has shown that BCSA cement concrete and PC concrete have similar compressive strengths, but the rate of strength gain, shrinkage, and creep differ [15]. This project was performed as an addition to previous work investigating the flexural behavior of reinforced BCSA cement concrete beams [22]. The original work tested early age members only and did not investigate the long-term behavior of the beams. Short-term and long-term shear strengths were investigated in this study.

2.2 Shear Capacity Prediction Equations

Due to the complexity of shear strength and behavior, there has been much research done to develop equations for the shear capacity of reinforced and prestressed concrete. The shear capacity of a reinforced concrete beam is dependent on the dimensions and geometry of the beam, how the beam is loaded, and the structural properties of the concrete and reinforcing steel [23]. There are five main parameters affecting shear strength for concrete beams without shear

reinforcement: compressive strength of the concrete, size effect, shear span to depth ratio, longitudinal reinforcement ratio, and axial force [23].

Unlike flexural strength, classical beam theory does not always apply to shear strength and behavior. There are two types of cracking in shear, web-shear cracking, and flexural-shear cracking as seen in Figure 1. Web-shear cracks develop in the web due to the principal tension stresses in the web perpendicular to the inclined compression strut. Flexural-shear cracks form as flexural cracks due to bending and change directions where the inclined tension stresses exceed the tensile strength of the concrete.

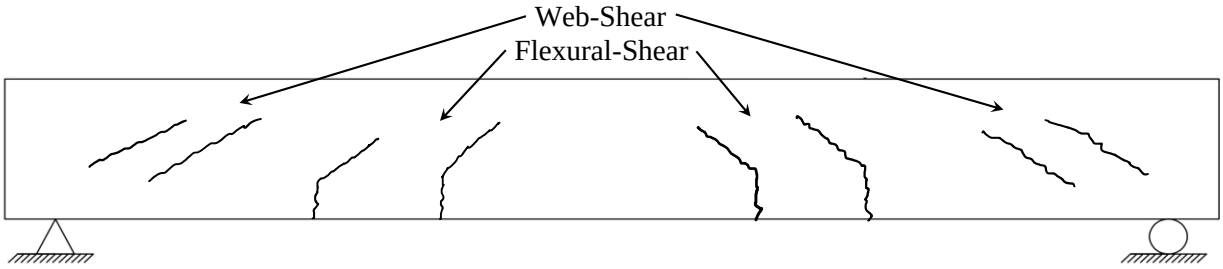

Figure 1. Types of Shear Cracks

2.2.1 ACI 318-14

ACI divides nominal shear capacity (V_n) into two parts; shear capacity of transverse reinforcement (V_s) and shear capacity of the concrete (V_c). Since the tested beams had no transverse reinforcement, V_n is equal to V_c. The ACI code limits f'_c to 10,000 psi because there is limited shear research for higher concrete strengths.

2.2.1.1 Detailed method

In equations "(a)" and "(b)", shown in Table 1, there are two terms that are then multiplied by the effective area. The first term is a factor of the square root of f'_c. This term is

based on an empirical relationship between a concrete's compressive strength and its tensile strength. The second term is described as consisting of multiple properties that affect shear strength in a member [7]. The ρ_w is used to account for the longitudinal reinforcement's contribution to the shear strength and $\frac{V_u d}{M_u}$ accounts for the reduction in shear capacity in regions of large bending moment.

Table 1. Detailed method for calculating V_c, adapted from ACI 318-14 Table 22.5.5.1

V_c		
Least of (a), (b), and (c):	$\left(1.9\lambda\sqrt{f_c'} + 2500\rho_w \frac{V_u d}{M_u}\right) b_w d$	(a)
	$\left(1.9\lambda\sqrt{f_c'} + 2500\rho_w\right) b_w d$	(b)
	$3.5\lambda\sqrt{f_c'} b_w d$	(c)

Therefore, the equations for the detailed method of calculating the shear capacity provided by the concrete account for the concrete's tensile strength, strength added due to the longitudinal reinforcement, and the ratio of the shear and moment in the section being analyzed.

2.2.1.2 Simplified method

$$V_c = 2\lambda\sqrt{f_c'} b_w d \qquad \text{ACI 318-14 Equation 22.5.5.1}$$

ACI 318-14 offers a simplified method of calculating the shear capacity provided by the concrete in a reinforced concrete member with no transverse shear reinforcement. This simplified equation, "ACI 318-14 Equation 22.5.5.1", assumes that the second term, in the above equations "(a)" and "(b)", which corresponds to the longitudinal reinforcement's contribution to shear strength and shear to moment ratio, is equal to $0.1\lambda\sqrt{f_c'}$. This assumption is conservative and is said to be applicable for most designs.

2.2.2 ACI 318-19

ACI 318-19 added consideration for the size-effect, λ_s. Kuchma et al. 2019 [24] found that for nonprestressed members without shear reinforcement, the shear strength does not increase in direct proportion with member depth. Table 2 shows the current equations for shear strength of concrete members in ACI 2019. The current approach is broken up into two sections, one section where the shear reinforcement provided is greater than the code-defined minimum, and one where the shear reinforcement provided is less than the code-defined minimum. The second term in each of the equations accounts for the change in shear strength attributed to axial loads where N_u is the axial load, positive for compression and negative for tension. In ACI 318-14, the shear strength attributed to the tensile strength of the concrete and the shear strength attributed to the longitudinal reinforcement steel were in two separate terms, and the shear strength for axially loaded members was determined using a separate equation. In ACI 318-19, the axial load term is always considered, and, unlike ACI 318-14, axial tension is accounted for if present. In addition to the previously stated change, ACI 318-19 combines the terms for tensile strength of concrete and the strength attributed to the longitudinal reinforcement into one term in equations "(b)" and "(c)." Equation "(c)" accounts for the previously described size-effect factor and equation "(a)" is a simplification of equation "(b)" and is allowed to be used instead of equation "(b)." In this research, no reinforcement was used, therefore equation (c) was used to calculate the shear strength of the beams.

Table 2. V_c for nonprestressed members, adapted from ACI 318-19 Table 22.5.5.1

Criteria	V_c		
$A_v \geq A_{v,min}$	Either of:	$\left[2\lambda\sqrt{f_c'} + \frac{N_u}{6A_g}\right] b_w d$	(a)
		$\left[8\lambda(\rho_w)^{\frac{1}{3}}\sqrt{f_c'} + \frac{N_u}{6A_g}\right] b_w d$	(b)
$A_v < A_{v,min}$	$\left[8\lambda_s\lambda(\rho_w)^{\frac{1}{3}}\sqrt{f_c'} + \frac{N_u}{6A_g}\right] b_w d$		(c)

2.2.3 AASHTO LRFD

The AASHTO shear capacity equations are largely based on the Modified Compression Field Theory (MCFT). V_n is to be taken as the lesser of "AASHTO LRFD 2017 Equation 5.7.3.3-1 and 5.7.3.3-2." This limit is in place to ensure that the concrete in the web of the beam does not crush prior to the transverse steel yielding. The term α is defined as the angle measured from the longitudinal reinforcement to the transverse reinforcement. By this definition, vertical shear reinforcement would have an α = 90°. θ is the angle of inclination of the diagonal compressive stresses where the crack would form; in other words, it corresponds to the angle of the shear crack at a section. β accounts for the cracked concrete's ability to transfer tension and shear. The beams in this study had an overall depth less than 16 in. Therefore, AASHTO permits the use of β = 2.0 and θ = 45 degrees.

$$V_n = V_c + V_s + V_p \qquad \text{AASHTO LRFD 2017 Equation 5.7.3.3-1}$$

$$V_n = 0.25 f_c' b_v d_v + V_p \qquad \text{AASHTO LRFD 2017 Equation 5.7.3.3-2}$$

$$V_c = 0.0316 \beta \lambda \sqrt{f_c'} b_v d_v \qquad \text{AASHTO LRFD 2017 Equation 5.7.3.3-3}$$

$$V_s = \frac{A_v f_y d_v (\cot\theta + \cot\alpha)\sin\alpha}{s}$$ AASHTO LRFD 2017 Equation 5.7.3.3-4

2.2.4 Eurocode 2

"Eurocode 2 Equation 6.2a" is used to calculate the shear strength of concrete members with no transverse shear reinforcement. It is recommended to take $C_{Rd,c} = 0.18/\gamma_c = 0.12$ when $\gamma_c = 1.5$, $k_1 = 0.15$. The first term in "Eurocode 2 Equation 6.2a" accounts for the tensile strength of the concrete and accounts for the shear strength contributed by the longitudinal reinforcement. The contribution from the longitudinal steel is limited to a reinforcement ratio less than 0.02. The second term accounts for an axial force applied to the member where compression is positive and increases strength and tension is negative and decreases strength.

$$V_{Rd,c} = \left[C_{Rd,c} k (100\rho_l f_{ck})^{\frac{1}{3}} + k_1 \sigma_{cp}\right] b_w d$$ Eurocode 2 Equation 6.2a

$$V_{Rd,c.min} = \left(v_{min} + k_1 \sigma_{cp}\right) b_w d$$ Eurocode 2 Equation 6.2b

$$k = 1 + \sqrt{\frac{200}{d}} \leq 2.0$$

$$\rho_l = \frac{A_{sl}}{b_w d} \leq 0.02$$

$$\sigma_{cp} = \frac{N_{Ed}}{A_c} < 0.2 f_{cd}$$

$$v_{min} = 0.035 k^{3/2} (f_{ck})^{1/2}$$

2.2.5 SMCFT

SMCFT is based on the Compression Field Theory (CFT). In CFT, it is assumed that a diagonal "compression field" in the uncracked concrete carries shear forces after cracking [23]. The compatibility equations are as follows.

$$f_2 = v(\tan\theta + \cot\theta) \qquad \text{NCHRP Equation A-5a}$$

$$\rho_x f_{sx} = v\cot\theta \qquad \text{NCHRP Equation A-5b}$$

$$\rho_v f_{sy} = v\tan\theta \qquad \text{NCHRP Equation A-5c}$$

Theta is the angle of inclination of the compression strut, which is also the angle of the shear cracks. A steep angle of inclination means the longitudinal strain is high, and a shallow angle of inclination means the transverse strain is high [23]. CFT assumed a bilinear relationship between the stress and strain for both longitudinal and transverse reinforcement [23].

$$f_2 = \left(\frac{f'_c}{\varepsilon'_c}\right)\varepsilon_2 \le f_{2,max} = \frac{3.6f'_c}{1+2(\varepsilon_1+\varepsilon_2)/\varepsilon'_c} \qquad \text{NCHRP Equation A-14}$$

After CFT was developed, many researchers studied its applicability. Through experimental testing, Vecchio and Collins further refined "NCHRP Equation A-14" which resulted in the following "NCHRP Equation A-18."

$$f_2 = f_{2,max}\left[2\left(\frac{\varepsilon_2}{\varepsilon'_c}\right) - \left(\frac{\varepsilon_2}{\varepsilon'_c}\right)^2\right] \qquad \text{NCHRP Equation A-18}$$

CFT has been shown to predict shear behavior for any type of loading and gives a conservative estimate of the strength of the member. Hawkins et al. [23] attributes this to CFT's "equilibrium conditions, compatibility conditions, and constitutive relationships for both

reinforced and cracked concrete." CFT does not consider the tensile stresses in cracked concrete which is what led to the development of the Modified Compression Field Theory (MCFT). The MCFT equilibrium equations are very similar to CFT, with the addition of concrete tensile stresses.

$$\rho_x f_{sx} = v\cot\theta - f_1 \qquad \text{NCHRP Equation A-19a}$$

$$\rho_v f_{sy} = v\tan\theta - f_1 \qquad \text{NCHRP Equation A-19b}$$

$$f_2 = v(\tan\theta + \cot\theta) - f_1 \qquad \text{NCHRP Equation A-19c}$$

Where f_1 is the tensile stress in the concrete described by Hawkins et al 2005 as follows [23].

$$f_1 = \frac{f_{cr}}{1+\sqrt{500\varepsilon_1}} = \frac{4\sqrt{f'_c}}{1+\sqrt{500\varepsilon_1}} \text{ (psi)} \qquad \text{NCHRP Equation A-20}$$

CFT and MCFT are both useful for predicting shear strength of members with transverse reinforcement. When there is not transverse reinforcement, the CFT provides a conservative shear strength due to its omission of the contribution to shear capacity of the concrete tensile strength. Therefore, the MCFT can predict shear behavior and strength of members without shear reinforcement.

The next development in CFT came from Bentz et al. [10] with the development of the SMCFT. When MCFT was adopted by AASHTO it was implemented as a set of tables which required an iterative process to select design values. The process was criticized by designers for being too complicated and for the underlying theory behind them not being clear in the design process [10]. The simplification of the MCFT was made so that engineers could have access to a

quick and easy method of accurately calculating shear strength of typical reinforced concrete members and be able to understand the calculations being performed [10].

The general process for the Simplified Modified Compression Field Theory (SMCFT) is rather simple. It is important to note that the solution is an iterative one based on strain and the following example of the calculation is based on a member with no transverse reinforcement, thus $v_s = 0$. The first equation is as follows:

$$v = v_c + v_s = \beta\sqrt{f_c'} + \rho_z f_y cot\theta \qquad \text{Bentz et al. Equation 18}$$

It can be seen that the shear strength of the concrete relies on the factor β and the square root of the compressive strength of the concrete, f'_c. Historically, a factor multiplied by the "nth" root of the compressive strength of concrete has been correlated with the tensile strength of the concrete. This is no different in the SMCFT except in SMCFT β, for members with no transverse reinforcement, is calculated using "Bentz et al. Equation 27."

$$\beta = \frac{0.4}{1+1500\varepsilon_x} \cdot \frac{1300}{1000+s_{xe}} \qquad \text{Bentz et al. Equation 27}$$

In "Bentz et al. Equation 27", ε_x is the strain that is selected to begin the iterative process. Bentz et al. suggests a value of 0.001 to be used to start. The crack spacing parameter, or s_{xe}, is calculated using "Bentz et al. Equation 22."

$$s_{xe} = \frac{35s_x}{a_g+16} \qquad \text{Bentz et al. Equation 22}$$

In "Bentz et al. Equation 22", s_x is the crack control characteristic of the reinforcement in the x-direction (longitudinal reinforcement) and is taken as the distance from the top of the beam and the centroid of the longitudinal steel, or the effective depth of the steel. The last unknown in

"Bentz et al. Equation 22" is a_g, the maximum coarse aggregate size in the concrete mix. Note that this equation is developed for s_x and a_g in units of mm and it is specified that if $f'_c > 70$ MPa or 10,000 psi that a_g should be taken as zero since cracks tend to propagate through rather than around the coarse aggregate in high strength concretes.

Now that s_{xe} is calculated, and ε_x is assumed, the β factor can be calculated. With β and the already known compressive strength of the concrete, v_c (allowable shear stress) can be calculated per "Bentz et al. Equation 18." The shear strength contributed by the steel relies on the reinforcement ratio of the transverse reinforcement (ρ_z), the yield stress of the transverse reinforcement (f_y), and the inclination angle of the compression strut (θ). The concrete will crack along the compression strut, thus θ is also the crack inclination angle and calculated per "Bentz et al. Equation 28."

$$\theta = (29deg + 7000\varepsilon_x)\left(0.88 + \frac{s_{xe}}{2500}\right) \leq 75deg \quad \text{Bentz et al. Equation 28}$$

After theta is calculated, the longitudinal strain can be obtained by using "Bentz et al. Equation 29."

$$\varepsilon_x = \frac{v\cot\theta - v_c/\cot\theta}{E_s\rho_x} \quad \text{Bentz et al. Equation 29}$$

In "Bentz et al. Equation 29," E_s is the modulus of elasticity of the longitudinal steel and ρ_x is the longitudinal reinforcement ratio. E_s is in units of MPa. With the new longitudinal strain calculated, the process is then repeated until the longitudinal strain converges to a solution. The allowable shear stress is then multiplied by the cross section of the beam to calculate the shear capacity.

2.3 Carbonation

Carbonation in PC is a process in which carbon dioxide (CO_2) enters the concrete and reacts with calcium hydroxide ($Ca(OH)_2$) in the cement paste [25]. This reaction, which produces calcium carbonate ($CaCO_3$) and water (H_2O), consumes calcium hydroxide ions, and lowers the pH of the concrete [26]. Corrosion of reinforcement in concrete can occur if the pH is not sufficiently high to passivate the steel. This is detrimental to the strength and safety of the member. A common method to determine the depth of carbonation in concrete samples is the use of a pH indicator on a freshly exposed cross-section [26, 27]. Carbonation initially starts at the surface and may eventually reach the center of a concrete member. Carbonation can be seen clearly by a pH gradient from the surface of the concrete to the interior. The pH of PC concrete is generally 12-13 [28].

In contrast, carbonation in ettringite based binders such as BCSA cement is said to be faster than in PC due to the smaller amount of calcium hydroxide [29]. When calcium hydroxide reacts with CO_2 it slows its progression into the concrete. When there is less calcium hydroxide to react with, the CO_2 permeates into the concrete matrix at a faster rate [29]. In addition to the faster rate of carbonation, instead of densifying the paste, carbonation has led to an increase in porosity which decreases the strength of the concrete [29].

3. Experimental procedure

3.1 Mix proportioning

A commercially available BCSA cement was used, and its performance was compared with Type I/II PC. The mix design used by Cook et al. [22] was used for this study to ensure consistency with past work on structural concrete made with BCSA cement. A target mixture temperature of 65°F-75°F was established. Because of this, days prior to mixing, materials were

gathered and stored in air-tight containers which were placed in a climate-controlled room with a temperature of 72°F. Samples of coarse and fine aggregate were taken and dried in an oven to calculate the moisture contents per ASTM C556-19 [30].

High summertime temperatures and mixing in an unconditioned environment required the use of ice to control the temperature of the BCSA cement concrete mixtures. A relationship was established between the mix temperature (T_m) and the following ratio:

$$\frac{\left(T_{wi}*\frac{w}{c}\right)+T_a}{2}$$

Where T_{wi} is the initial temperature of the water (°F), w/c is the water-cement ratio, and T_a is the expected ambient temperature in °F.

The weight of ice needed was based off the temperature of the water (starting energy) and the desired mixture temperature. Calculations were based off the specific heat of water at 70°F (4.178 J/(g-K)) for all starting temperatures and the specific heat of ice at 32°F (2.05 J/(g-K)). A linear trendline was fit to the initial data points. As more mixes were performed, more data was gathered, the calculator became more accurate and the equation of the trendline changed as shown in Figure 2. The calculated weight of ice was directly substituted for the equivalent weight of water. The performance of the calculator was deemed satisfactory, and the temperature of the mixtures were within the desired range.

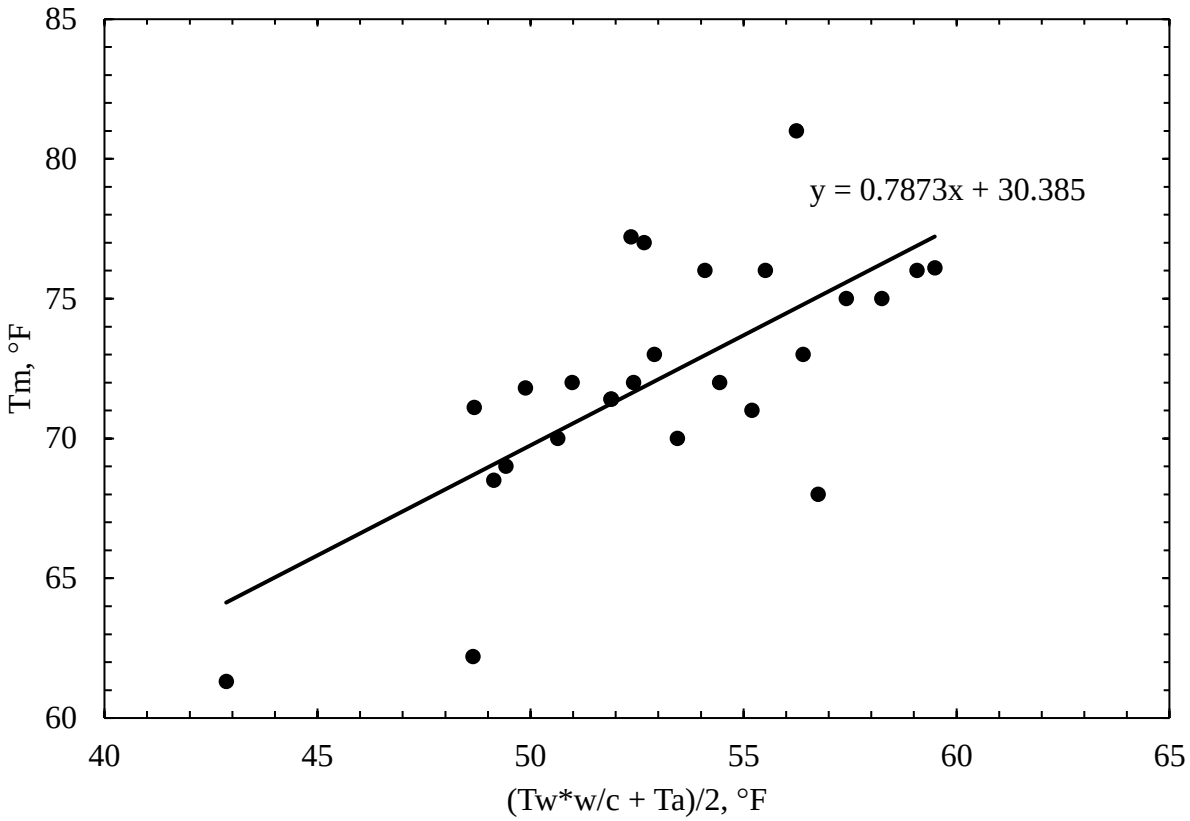

Figure 2. Ice calculation relationship plot

A polycarboxylate based high range water reducer (HRWR) was used in both BCSA cement and PC mixes. This allowed for an increased workability so that the mixture could be consolidated within the forms easily and quickly. In addition to HRWR, the fast-setting nature of BCSA cement concrete required the use of a set retarder for adequate working time. Citric acid has been shown to effectively slow the setting time without negatively affecting the compressive strength [3]. For this work, a solution of 5 lbs. powdered food grade citric acid per gallon of water was used as an admixture. A 9 fl. oz. per 100 lbs. cement dosage of this admixture was used, corresponding to 0.35% citric acid by cement weight. This dosage has been shown in the past to provide around 40 minutes of working time [5]. Mix proportions are presented in Table 3 for the BCSA cement and PC concrete beams. The mix design was developed so that a similar

amount of cement and aggregate would be used in each mix. The differences in weights of materials are associated with differing w/c and specific gravity of the cements.

Table 3. Proportions of Materials, per yd^3

Cement Type	Cement, lbs	Coarse Aggregate, lbs	Fine Aggregate, lbs	Water, lbs	Assumed Air Content, %	HRWR, fl. oz. per CWT	Citric Acid, % CWT	w/c
BCSA	658	1782	1156	316	1.5	18	0.35	0.48
PC	660	1775	1187	264	1.5	4	0	0.40

The coarse aggregate used in the mixtures was a 1 in. nominal maximum size aggregate (NMSA) crushed limestone. The gradation, fineness modulus, specific gravity, and absorption for the coarse aggregate are found in Table 4. The fine aggregate used was Arkansas River sand quarried in Van Buren, AR. The gradation, fineness modulus, specific gravity, and absorption are found in Table 5. The aggregate properties were determined using ASTM C127 and C128 [31, 32].

Table 4. Coarse Aggregate Gradation

Sieve Size	% Retained	% Passing
$1^1/_2$	0	100
1	0.39	99.61
$^3/_4$	10.75	89.25
$^1/_2$	35.98	64.02
$^3/_8$	52.56	47.44
4	84.45	15.55
8	94.95	5.05
16	96.17	3.83
30	96.49	3.51
50	96.72	3.28
100	97.93	3.07
200	97.22	2.78
Pan	97.38	2.62
Specific Gravity		2.567
% Absorption		2.3

Table 5. Fine Aggregate Gradation

Sieve Size	% Retained	% Passing
$^3/_8$	0	100
4	2.8	97.2
8	8.1	91.9
16	19.5	80.5
30	39	61
50	83.2	16.8
100	97.9	2.1
200	99.3	0.7
Pan	99.4	0.6
Fineness Modulus		2.51
Specific Gravity		2.63
% Absorption		0.55

3.2 Beam design

The beams were designed to fail in shear rather than in flexure. Each beam was 6 in. (152 mm) wide, 12 in. (305 mm) tall, and 8 ft. (2.4 m) long. To ensure a shear failure, the beams were designed to support a single point load near one end (24 in. from support) with a shear span to depth ratio of 2.0. Based on this load location, failures would be expected to be at a higher load. The beams were designed using the simple V_c equation from ACI 318-14, and a 28-day compressive strength of 7,000 psi was assumed.

Two grade 60 #5 rebars with standard hooks (l_{ext} = 7.5 in), designed per ACI 318-14 [11], were placed with 1 in. (25mm) of clear cover on all sides. The effective depth, d, was 10.69 in. This set up is represented in Figure 3. The design moment capacity of the beams was 378.19 kip-in, and the design shear capacity was 10.73 kip. A maximum point load of 16,000 lbf was predicted based on the location of the point load. This loading would exceed the shear capacity before the moment capacity was reached.

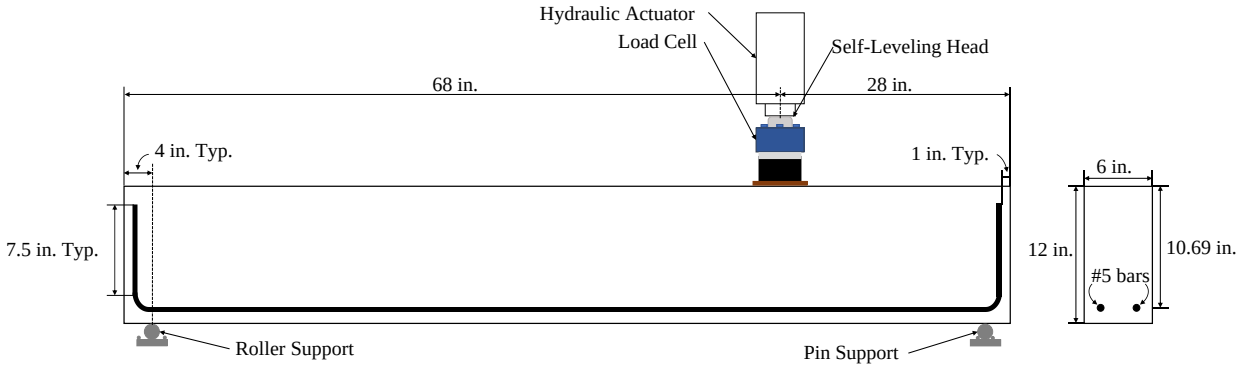

Figure 3. Beam Shear Testing Setup

3.3 Mixing and storing

A 20 cubic-foot capacity paddle mixer was used to make all the concrete in this research. The mix procedure was as follows: all of the sand, cement, and water (with admixtures added

into the mixing water) were added. This was mixed for thirty seconds and then the coarse aggregate was slowly added. This procedure was found to alleviate the mixer's tendency to bind up if all the coarse aggregate was added at once. Water temperature, ambient temperature, and mix temperature were measured and recorded for each mix. In addition to temperatures, the slump was measured for each mix per ASTM C143/C143M [33]. Two beams were cast out of each mixture to provide replicate samples. In the following sections of this thesis, the beams will be referred to as "Cement type-age-specimen number." For example, the first BCSA cement beam tested at 1 day of age was referred to as: "BCSA 1d-1." In these beam names, "h" was used for hours, "d" for days, and "y" for years.

The 3-hour, 1-day, and 28-day beams were stored inside a laboratory at the University of Arkansas Grady Harvell Civil Engineering Research and Education Center. The 1-year beams were stored outside at the University of Arkansas Engineering Research Center until tested. The 1-year beams were stored outside to expose them to weather and provide a realistic service environment for the future carbonation depth testing.

Differing numbers of cylinders were made for each cement type mix in order to perform compressive tests per ASTM C39/C39M [34]. Four sets of three cylinders were made for the BCSA cement mixes to be tested at 3 hours, 1 day, 28 days, and 1 year. Two sets of three cylinders were made for the PC mixes to be tested at 28 days and 1 year. The cylinders were demolded at the same time as the beams and placed into a water bath at a temperature of 72 degrees Fahrenheit.

3.4 Compression tests

Once cast, all PC companion cylinders sat next to the beams for one day at which time the cylinders were demolded and one day compressive strength tests were performed. For the

BCSA cement specimens, cylinders were demolded three hours after casting, and the BCSA 3-hour cylinders were tested. All other cylinders were then placed in a water bath at a temperature of 72°F until tested. Prior to testing, the cylinders were placed in a grinder to create a smooth and even loading surface. The compression testing took place in a Forney VFD compression machine per ASTM C39/C39M [34]. The ultimate load was recorded and used to calculate the compressive stress in the cylinder at failure.

3.5 Shear tests

The experimental set up of this study differed from some previous studies [35, 36]. Omar et al. 2021 [35], while studying the shear behavior of lightweight self-consolidating concrete (SCC), loaded their beams with two point loads close to mid-span. All their beams failed in shear. Lima et al. 2021 [36] also had a loading geometry of two point loads near mid-span, but in contrast to Omar et al. [35], their point loads were further apart. Like Omar et al. [35], the beams in the aforementioned study all failed in shear. In this study a single point load was applied near the end of the beam in order to force a shear failure.

Four sets of BCSA beams and two sets of PC beams were tested at varying ages. The BCSA beams were tested in sets of two at 3 hours, 1 day, 28 days, and 1 year, while the PC beams (also sets of two) were tested at 28 days and 1 year. During testing, each beam was placed on a self-reacting load frame with a point load applied 24 in. (610mm) from one support. Two linear variable differential transformers (LVDT) were placed at the location of the point load, one on each side of the beam, to measure deflection. For the initial beam shear tests, PC 1y-1 and PC 1y-2, a bracket was screwed into each side of the beams at the location of the point load. The LVDTs would be placed on the load frame and the ends would rest on the aforementioned bracket. See Figure 4. For later tests, the LVDTs were attached to the hydraulic ram, and the

ends rested on a plate at the top of the concrete beam at the location of the point load, as seen in Figure 5.

Figure 4. Initial shear test set up

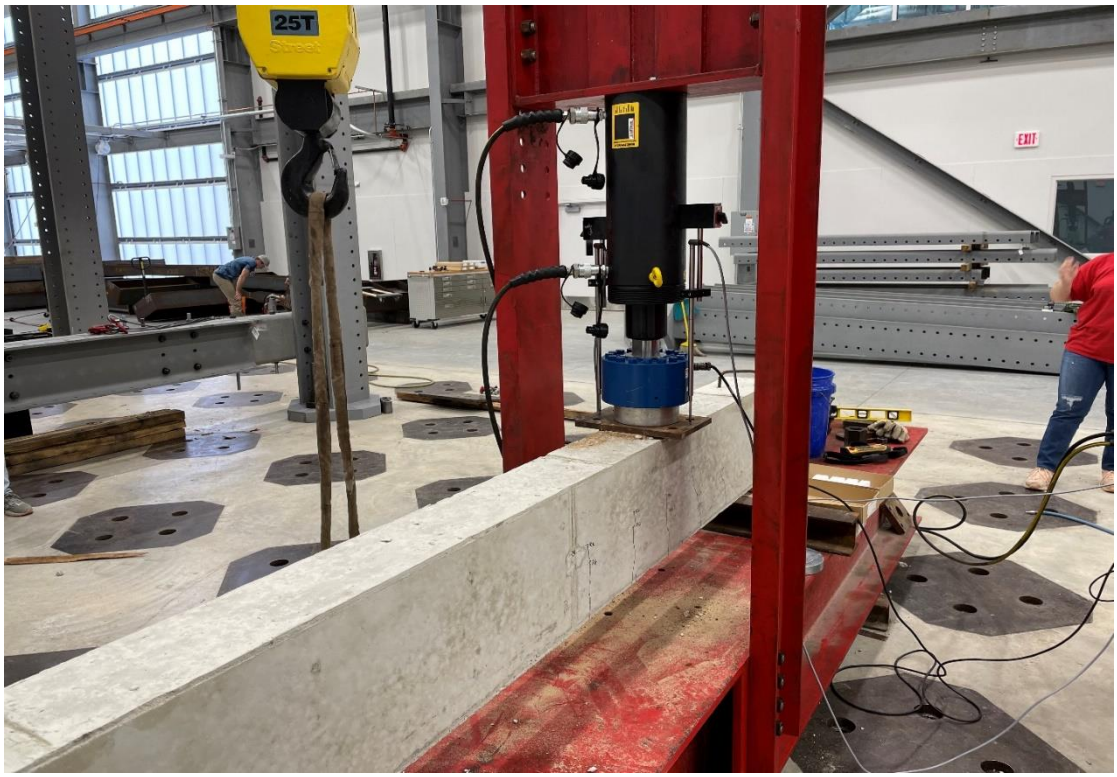

Figure 5. Refined set up

A hydraulic ram was used to apply the load. A load cell was placed between the beam and the hydraulic ram to measure the applied force. The beams were loaded in 2.5 kip (11 kN) increments up until significant shear cracking was present. In-between loading increments, cracks were identified and traced with a permanent marker. After significant cracking occurred, the beam was loaded gradually until failure. While the testing set up in this study varied from past studies, such as Omar et al. [35] and Lima et al. [36], the results and strength ratios were consistent between this study and the aforementioned studies.

3.6 Carbonation tests

Carbonation depth was determined by pH testing. A 1% (w/v) phenolphthalein indicator solution and Micro Essential Lab's Hydrion pH pencil was used, Figure 6. Phenolphthalein indicator changes colors to indicate pH. Phenolphthalein is colorless when the pH is below 9 and

it changes to a magenta color when the pH exceeds 9. The Microessentials pH pencil indicates a pH range of 0-13 by changing to various colors which can be correlated with an included identification card to determine the pH.

PC 1y-1, PC 1y-2, BCSA 1y-1, and BCSA 1y-2 were tested after being stored outside for more than 1 year. A concrete saw was used to cut cross-section slices out of the beams on the low-shear side of the beams. After cutting, the cross sections were brought indoors, the surfaces were wiped clean with a wet cloth, and pH testing was performed immediately. The pH indicators were applied at four locations on each cross-section: two locations on one edge along the depth of the beam and one location each on the top edge and bottom edge, as shown in Figure 7. After the indicator was applied, the carbonation depth was measured with digital calipers, recorded, and a picture was taken. The test locations are labeled one through four with an identifier in the following form, BCSA 1y-1 T1. This corresponds to test location one on the first one-year BCSA cement beam tested.

Figure 6. Phenolphthalein Solution and Microessentials Hydrion pH Pencil

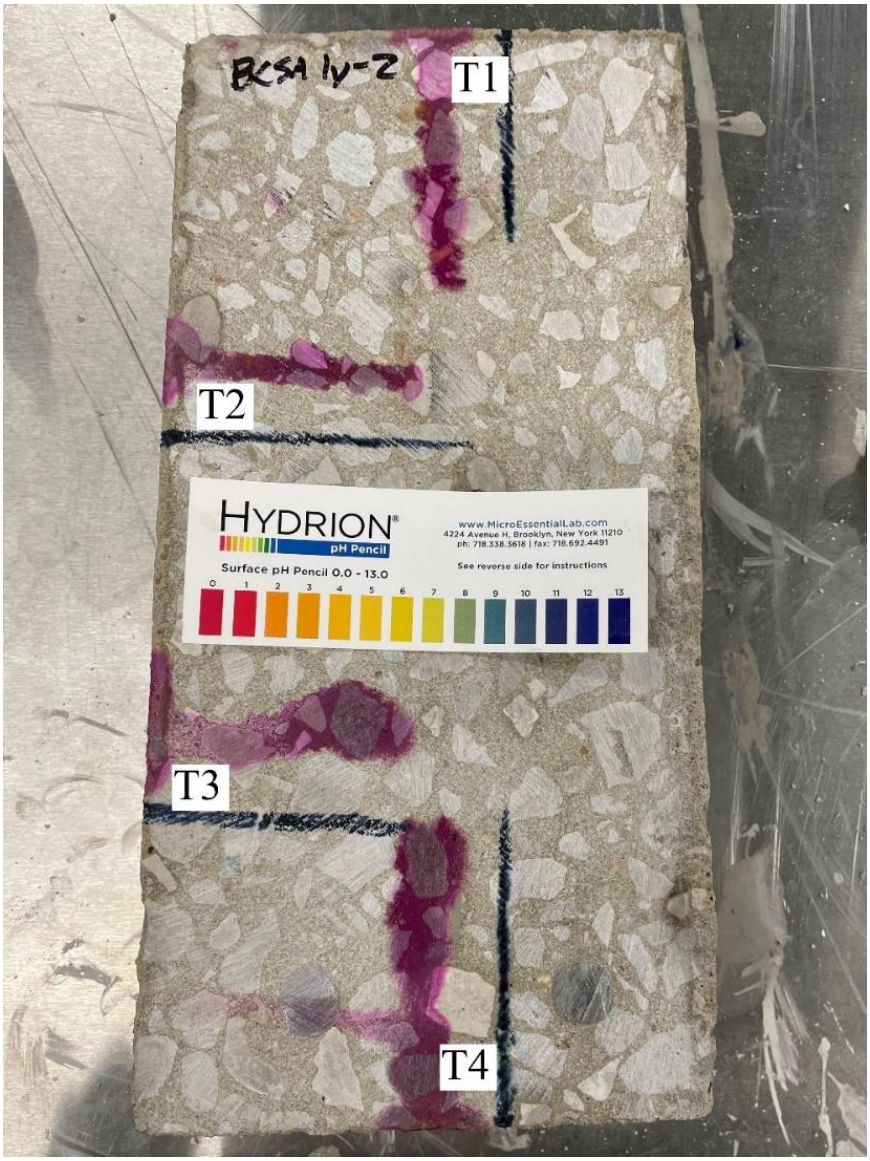

Figure 7. Test Locations

3.7 Long term compressive strength

To test the long term compressive strengths of BCSA cement and PC concrete beams, cores were cut out of the 1 year beam specimens after testing. The cores were cut into the sides of the beams in order to avoid the longitudinal reinforcement. Three cylindrical core samples were taken from each of the beams, the ends were ground, and their dimensions were measured

and recorded. The recorded compressive strengths were adjusted based on established criteria for cores in ASTM C24 [1].

Two length measurements were recorded for each cylinder, L_0 and L_{90}. L_0 is the initial length measurement and L_{90} is the length measured 90 degrees from the original measurement. Two diameter measurements were taken, D_0 and D_{90}. Each diameter measurement was taken at half height. D_0 is the initial diameter measurement and D_{90} is the measured diameter after the cylinder was rotated 90 degrees. The average of the lengths was divided by the average of the diameters to obtain the L_{avg}/D_{avg} ratio used to calculate the strength adjustment factor, C, per ASTM C42 [1]. Compression tests were performed per ASTM C39 and strength corrections made per ASTM C42 [1], [34]. Dimensions and strength adjustment factors, C, from ASTM C42 [1] can be found in Table 6. The cores from PC 1y-1 and PC 1y-2 were tested at 491 days of age and BCSA 1y-1 and BCSA 1y-2 at 471 days of age, respectively.

Table 6. Long-term compressive strength sample dimensions

Sample	L_0, in	L_{90}, in	D_0, in	D_{90}, in	L_{avg}, in	D_{avg}, in	L_{avg}/D_{avg}	A, in^2	C
PC 1y-1 1	5.701	5.703	3.747	3.746	5.702	3.747	1.522	11.02	0.962
PC 1y-1 2	5.878	5.888	3.740	3.736	5.883	3.738	1.574	10.97	0.966
PC 1y-1 3	5.854	5.854	3.751	3.743	5.854	3.747	1.562	11.03	0.965
PC 1y-2 1	5.922	5.926	3.740	3.742	5.924	3.741	1.584	10.99	0.967
PC 1y-2 2	5.952	5.932	3.747	3.735	5.942	3.741	1.588	10.99	0.967
PC 1y-2 3	5.926	5.923	3.747	3.746	5.925	3.747	1.581	11.02	0.967
BCSA 1y-1 1	5.799	5.814	3.747	3.747	5.807	3.747	1.550	11.03	0.964
BCSA 1y-1 2	5.727	5.739	3.748	3.747	5.733	3.748	1.530	11.03	0.962
BCSA 1y-1 3	5.795	5.795	3.748	3.747	5.795	3.748	1.546	11.03	0.964
BCSA 1y-2 1	5.713	5.710	3.744	3.751	5.712	3.748	1.524	11.03	0.962
BCSA 1y-2 2	5.802	5.801	3.749	3.747	5.802	3.748	1.548	11.03	0.964
BCSA 1y-2 3	5.890	5.855	3.748	3.744	5.873	3.746	1.568	11.02	0.965

4. Results

The data collected from each mix is detailed below in Table 8. The compressive strengths for the BCSA mixes were consistent throughout the study. PC-1y had higher compressive strengths than PC-28d. This difference was attributed to the higher mixture temperature and ambient temperature of PC-1y when compared to PC-28d. The higher mix temperature also helps to explain the lower slump. The compressive strengths in Table 7 are averages of three cylinder breaks per age.

Table 7. Compressive Strengths

Mix ID	Age	Average Compressive Strength, psi
BCSA 3h	3h	3930
	1d	5170
	28d	7910
	1y	-
BCSA 1d	3h	3540
	1d	4990
	28d	8010
	1y	-
BCSA 28d	3h	3140
	1d	4190
	28d	6740
	1y	-
BCSA 1y	3h	3760
	1d	4860
	28d	6600
	1y	8610
PC 28d	28d	7370
	1y	-
PC 1y	28d	10640
	1y	11750

Table 8. Mix Properties

Mix ID	Ambient Temperature, °F	Water Temperature, °F	Mix Temperature, °F	Slump, in
BCSA 3h	77	46	73	11
BCSA 1d	77	42	71	10
BCSA 28d	74	36	68	11
BCSA 1y	75	47	72	8.75
PC 28d	72	35	72	11
PC 1y	83	63	78	8.5

4.1 Shear testing results

A load versus deflection relationship was produced for each beam test. Figure 8 displays the general form of a load deflection plot generated in this study. The plots start with an initial slope. This slope changes two times over the course of the test. The first slope change correlates with the formation of a crack and a corresponding reduction in stiffness. The second slope change or the "plateau" occurs at the point when either the concrete crushed, or the steel yielded. This point was also taken as the "failure load" for purposes of shear strength calculation.

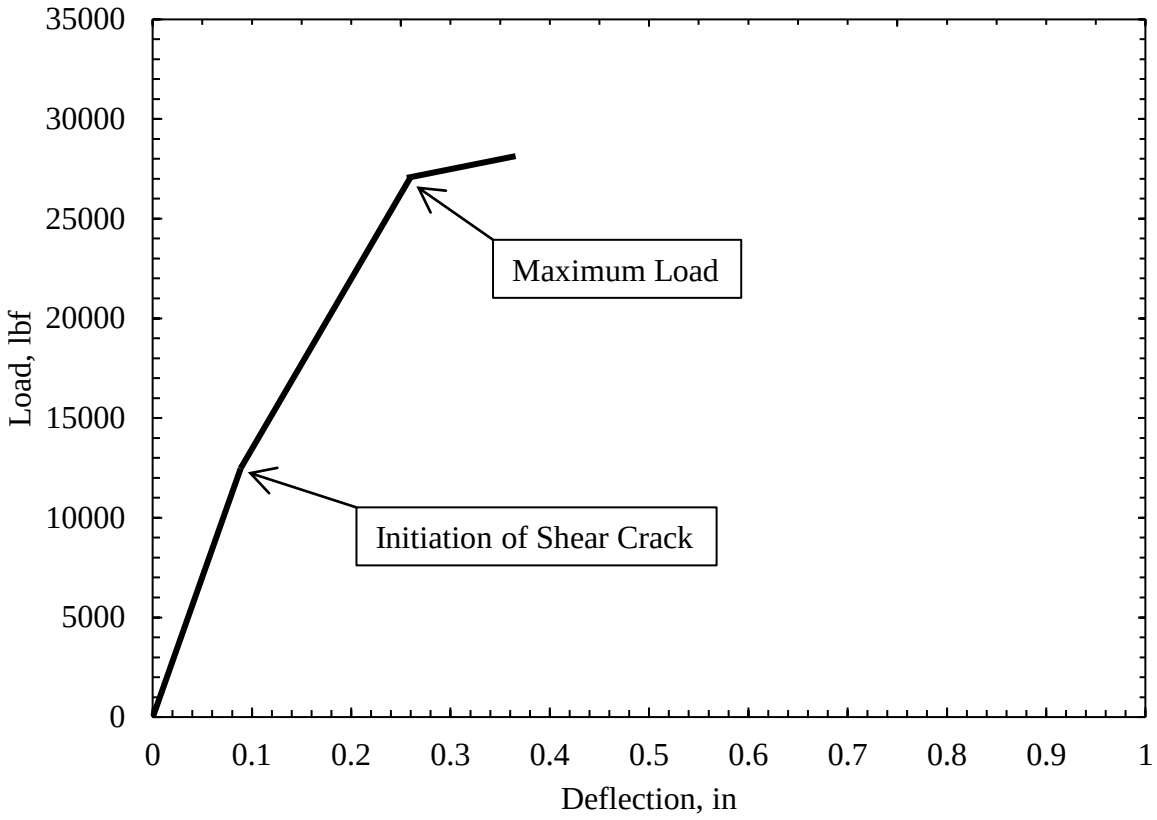

Figure 8. General form of load-deflection plots

4.1.1 BCSA beam shear test results

4.1.1.1 BCSA 3h-1 and BCSA 3h-2 beam shear test results

The 3-hour beams, BCSA 3h-1 and BCSA 3h-2, were poured on August 16th, 2021 and demolded approximately two hours later. For each beam, the first flexural cracks were recorded at a load of 7,500 lbf. The shear cracks for BCSA 3h-1 and BCSA 3h-2 appeared at 10,000 lbf and 12,500 lbf, respectively. Both tests resulted in shear failures with the first and second beams reaching an ultimate load of 14,685 lbf and 20,701 lbf, respectively. BCSA 3h-1 and BCSA 3h-2 were both loaded until there was a substantial drop in load, this occurred at a deflection of 0.45 in. for BCSA 3h-1 and 0.3 in. for BCSA 3h-2. For each beam, the concrete underneath the load

point crushed prior to failure. The load-deflection plot for BCSA 3h-1 and BCSA 3h-2 can be seen below as Figure 9.

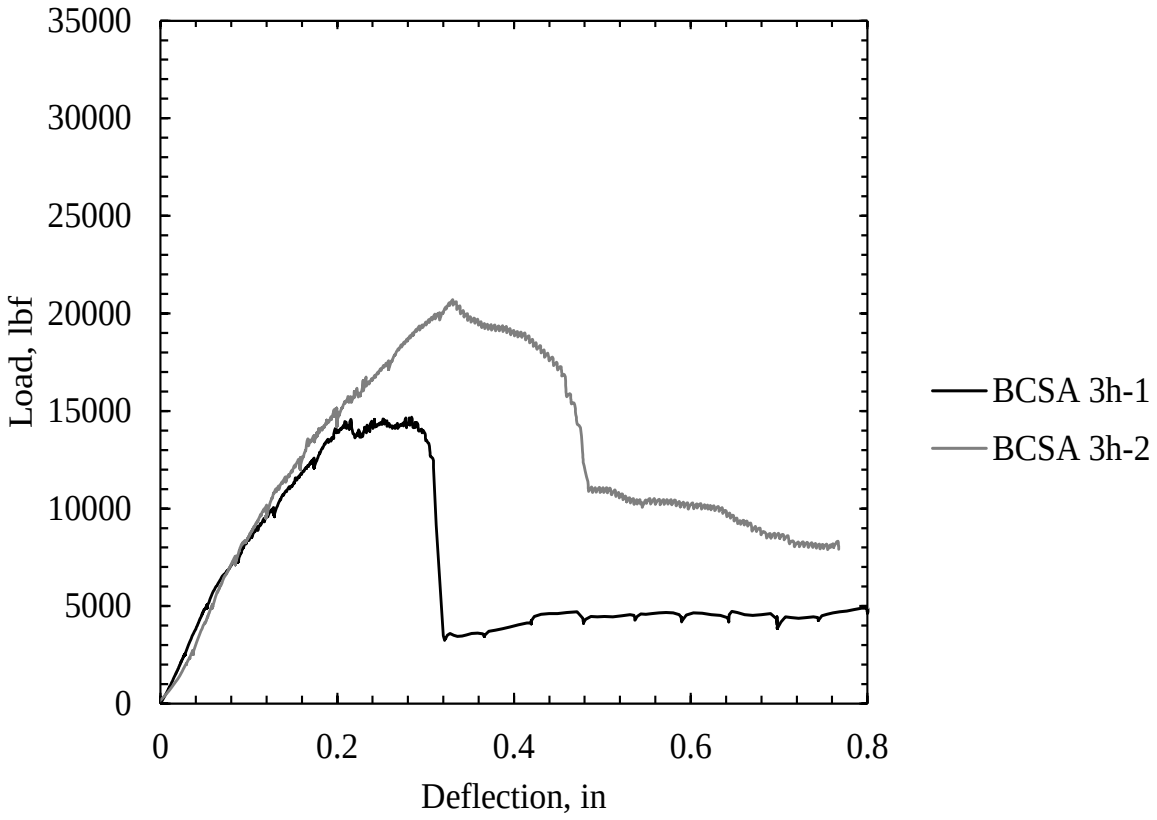

Figure 9. BCSA 3-hour load-deflection plot

4.1.1.2 BCSA 1d-1 and BCSA 1d-2 beam shear test results

The 1-day beams, BCSA 1d-1 and BCSA 1d-2, were poured on August 8th, 2021 and demolded one day later. For each beam, the first flexural cracks and the main shear crack were recorded at a load of approximately 7,500 lbf and 10,000 lbf, respectively. Both tests resulted in shear failures with the first and second beams reaching an ultimate load of 25,817 lbf and 24,607 lbf, respectively. Loading for BCSA 1d-1 was terminated after the peak load but before a substantial drop in load due to a malfunction in the testing equipment. The data that was collected was considered sufficient because a clear shear failure was observed and the load

carrying capacity of the beam was substantially reduced while the data recording equipment was functioning properly. The testing for BCSA 1d-2 ended after a substantial drop in load was witnessed. No crushing occurred before or after failure. The load-deflection plot for BCSA 1d-1 and BCSA 1d-2 can be seen below as Figure 10.

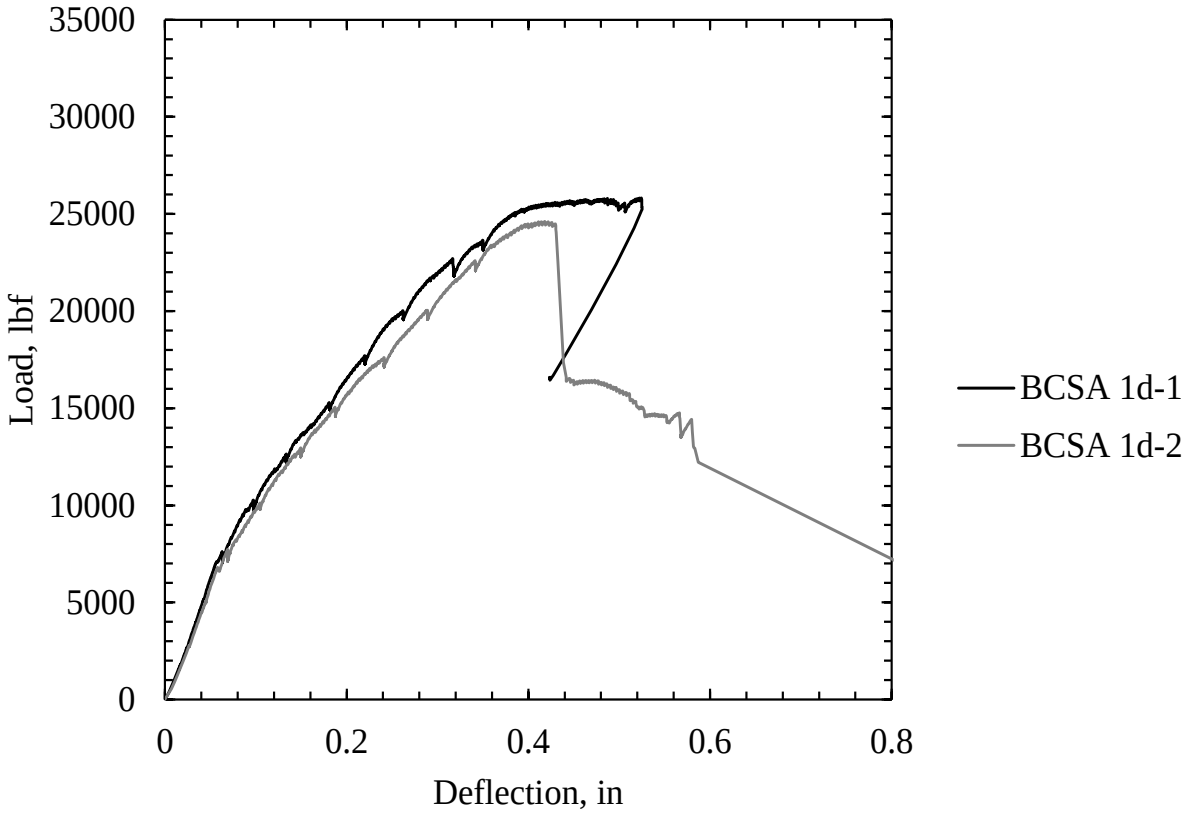

Figure 10. BCSA 1-day load-deflection plot

4.1.1.3 BCSA 28d-1 and BCSA 28d-2 beam shear test results

The 28-day beams, BCSA 28d-1 and BCSA 28d-2, were poured on June 9th, 2021 and tested July 7th, 2021. The first flexural cracks were recorded at a load of 10,000 lbf for both beams and shear cracks were observed at 15,000 lbf. Both tests resulted in a shear failure with the first and second beams reaching ultimate loads of 19,563 lbf and 26,743 lbf, respectively. Testing for BCSA 28d-1 was terminated when the applied load had plateaued. After the ultimate

load was reached for BCSA 28d-2, a bearing failure occurred at the hook location blowing off the end. This bearing failure occurred after the beam failed in shear. Crushing occurred underneath the load point for each beam. The load-deflection plot for BCSA 28d-1 and BCSA 28d-2 can be seen below as Figure 11.

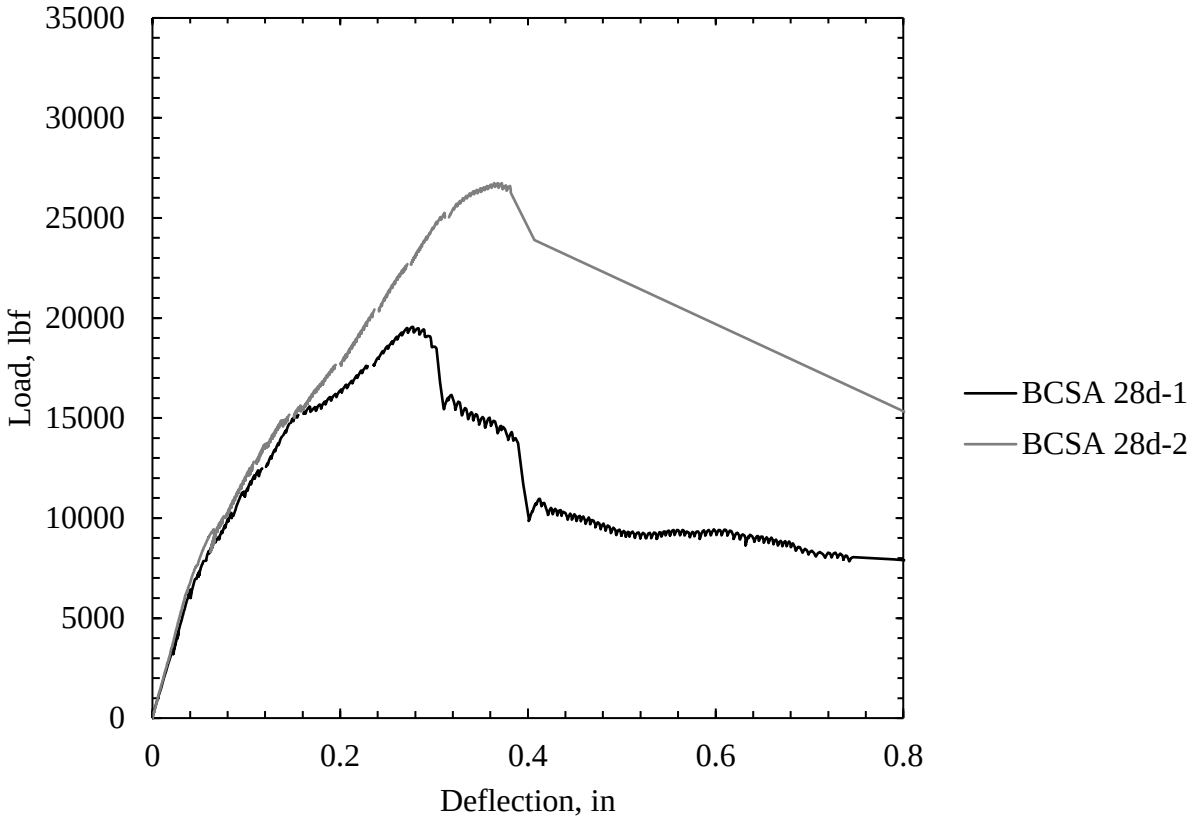

Figure 11. BCSA 28-day load-deflection plot

4.1.1.4 BCSA 1y-1 and BCSA 1y-2 beam shear test results

The 1-year beams, BCSA 1y-1 and BCSA 1y-2, were poured on July 20th, 2020 and tested July 20th, 2021. The first flexural cracks were recorded at a load of 10,000 lbf and shear cracks at 15,000 lbf. Both tests resulted in a shear failure with the first and second beam reaching an ultimate load of 26,261 lbf and 25,047 lbf, respectively. Testing for both beams was terminated shortly after reaching the ultimate loads with evidence that the beams had no

remaining load carrying capacity. Crushing was observed in each of the BCSA 1y beams underneath the load point. The load-deflection plot for BCSA 1y-1 and BCSA 1y-2 can be seen below as Figure 12.

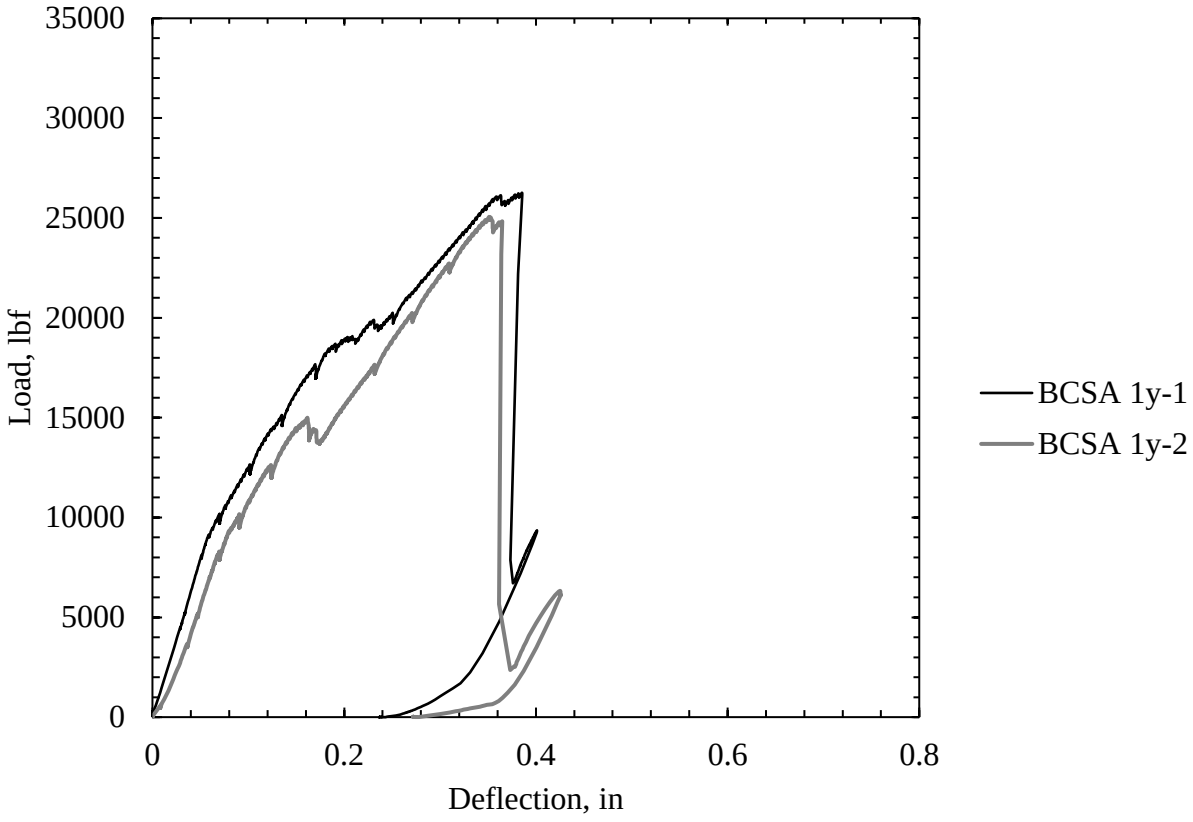

Figure 12. BCSA 1-year load-deflection plot

4.1.2 PC beam shear test results

4.1.2.1 PC 28d-1 and PC 28d-2 beam shear test results

The 28-day beams, PC 28d-1 and PC 28d-2 were poured on July 23rd, 2021 and tested August 20th, 2021. The first flexural cracks were observed at a load of 7,500 lbf for both beams. Both tests resulted in shear failures with PC 28d-1 failing at a maximum load of 28,357 lbf and PC 28d-2 at 27,050 lbf. Testing for PC 28d-1 was terminated after the concrete in the compression zone crushed resulting in a steep drop in load. Testing for PC 28d-2 was terminated

after a significant period of deflection without significant load gain. Crushing of concrete was observed in PC 28d-1 but not in PC 28d-2. The load-deflection plot for PC 28d-1 and PC 28d-2 can be seen below as Figure 13.

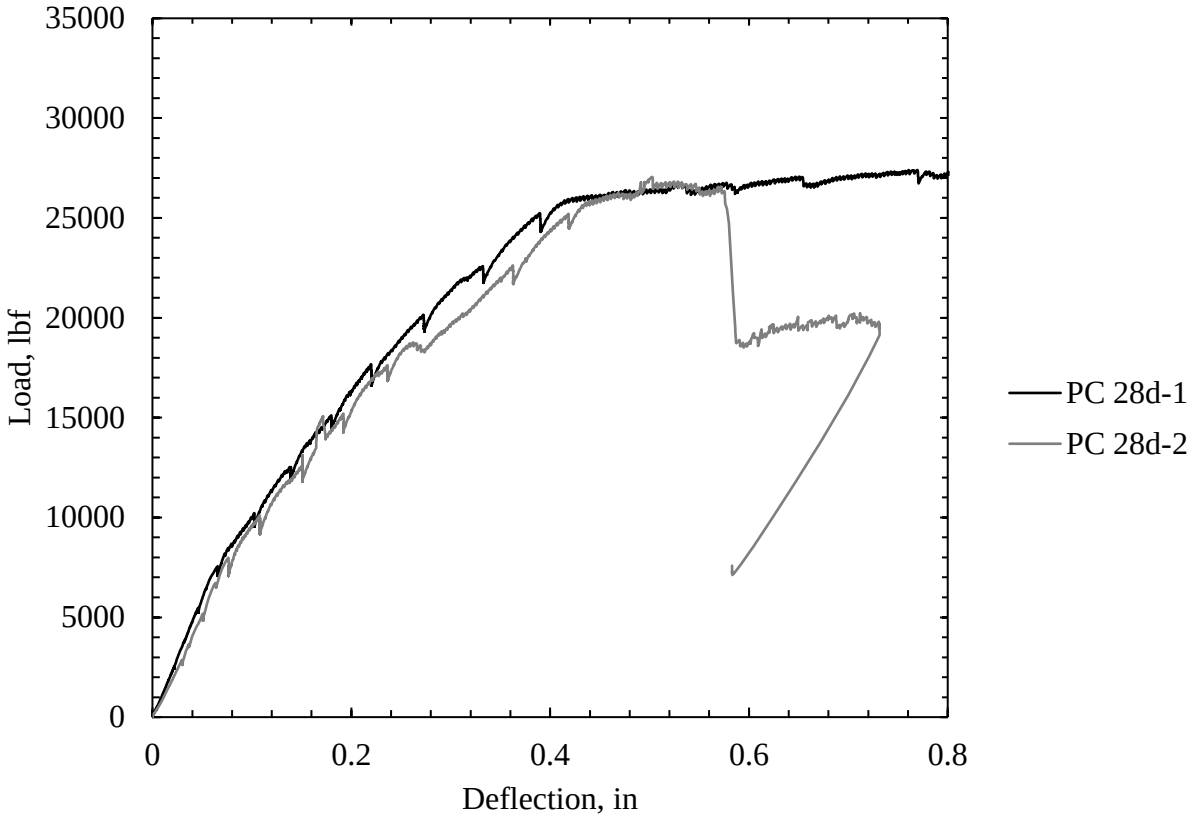

Figure 13. PC 28-day load-deflection plot

4.1.2.2 PC 1y-1 and PC 1y-2 beam shear test results

The 1-year beams, PC 1y-1 and PC 1y-2, were poured on June 30th, 2020 and tested July 28th, 2021. The first flexural cracks were documented at a load of 10,000 lbf for both beams. Both tests resulted in shear failures with PC 1y-1 failing at a maximum load of 27,927 lbf and 30,481 lbf for PC 1y-2. Both tests were terminated after a significant period of deflection without significant load gain. Crushing was observed underneath the load point in both PC 1y-1 and PC 1y-2. The load-deflection plot for PC 1y-1 and PC 1y-2 can be seen below as Figure 14.

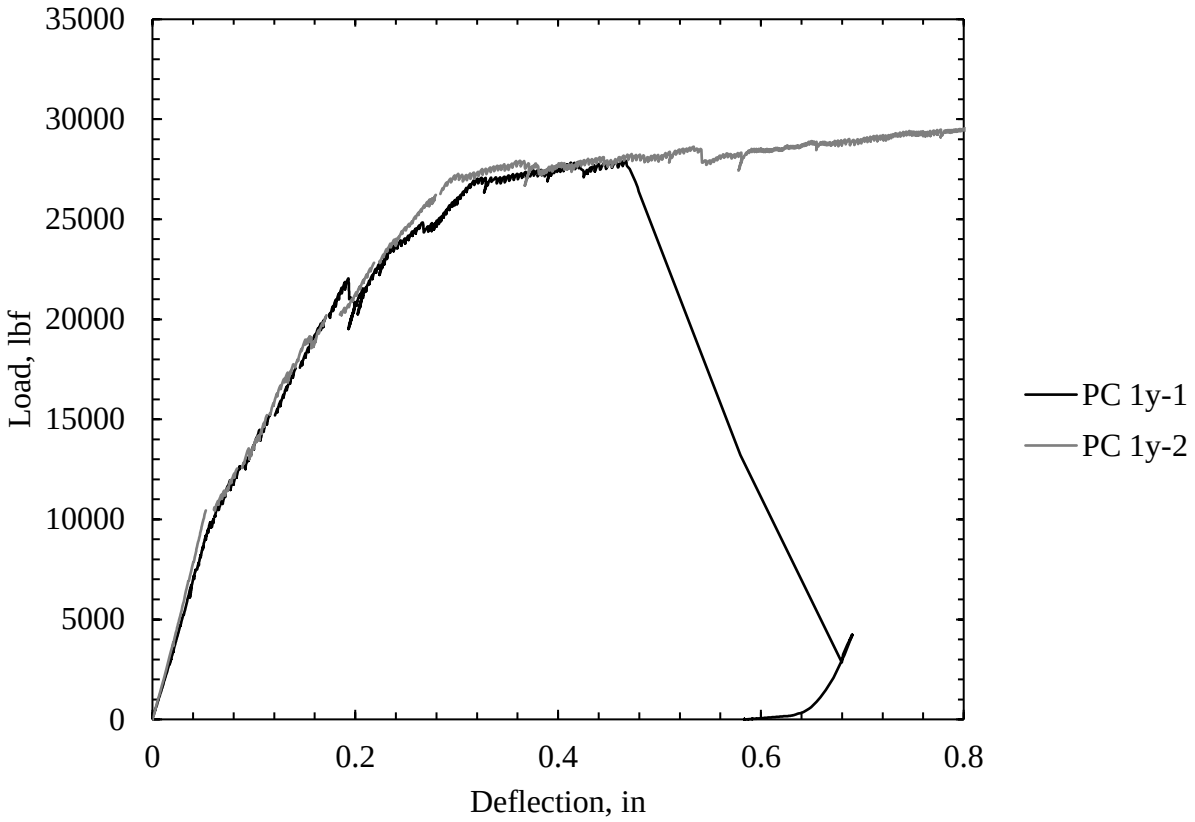

Figure 14. PC 1-year load-deflection plot

4.2 Carbonation testing results

The PC beams were tested on October 29th, 2021 at an age of 485 days. They were stored outside for 12 months in varying weather conditions of rain, heat, cold, and snow. After 12 months they were stored in a laboratory environment for the remaining 4 months before being tested. Upon first examination of the cross-sections of the tested PC beams, PC 1y-1 and PC 1y-2, there was no visible corrosion of the longitudinal reinforcing steel. The average of the measured clear cover for PC 1y-1 and PC 1y-2 are 0.760 in and 0.870 in, respectively. The pH indicators, phenolphthalein and Microessentials pH pencil, did not show any change in pH in the cross section and displayed a pH of 12. Therefore, there was no visually detectible carbonation front in the PC beams. Images of the cross sections can be seen in Figure 15 and Figure 16.

Figure 15. Carbonation test for PC 1y-1

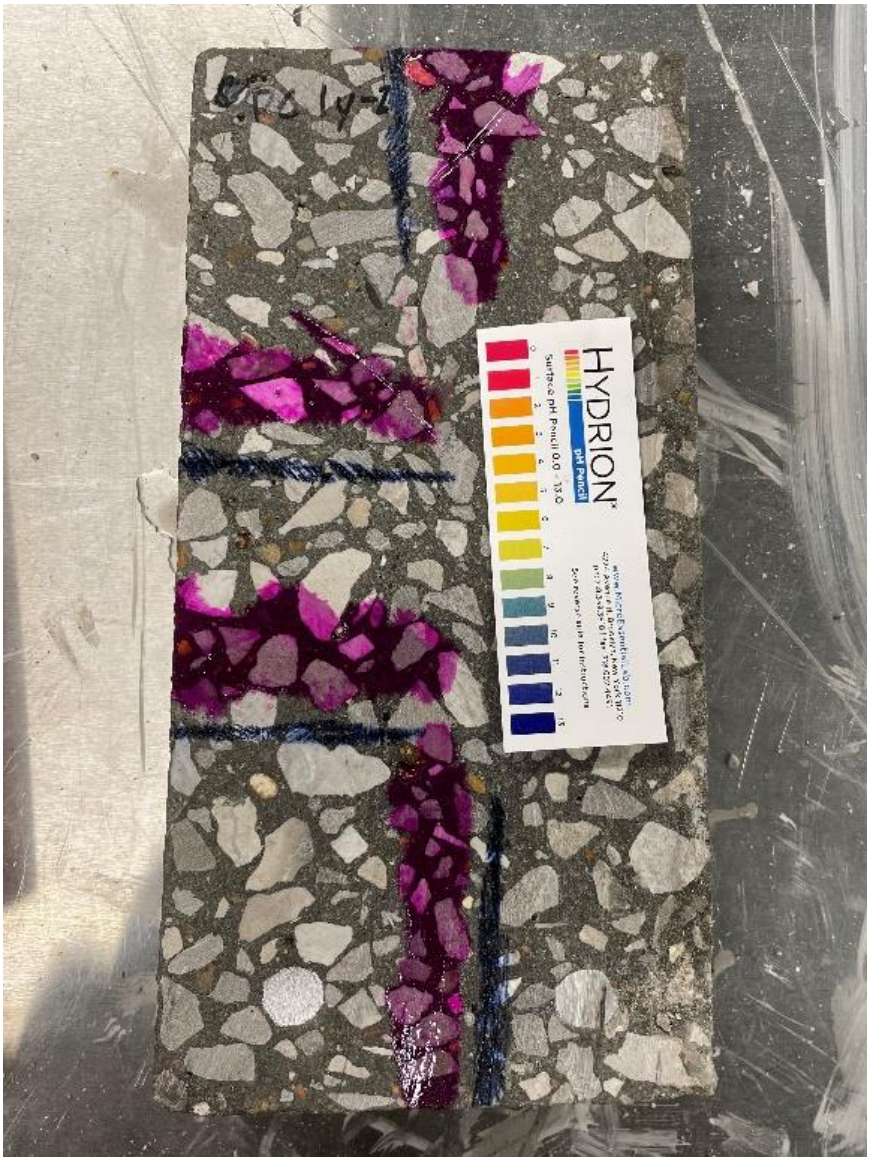

Figure 16. Carbonation test for PC 1y-2

The BCSA beams were tested on October 29, 2021 at 466 days old. They had been stored outside for 12 months in weather ranging from high heat to snow drifts and moved inside to a lab condition for the remaining 3 months. No corrosion was visibly noticeable in the longitudinal reinforcing steel of the tested BCSA beams, BCSA 1y-1 and BCSA 1y-2. BCSA 1y-1 had an average measured clear cover of 0.890 in and BCSA 1y-2 had an average measured clear cover of 0.995 in. The phenolphthalein solution did not show a change in pH for any test location. The

Microessentials pH pencil did not indicate any pH change in any test location. By using the included color chart, the pH of the concrete was 11-12. Images of the cross sections can be seen in Figure 17 and Figure 18.

Figure 17. Carbonation test for BCSA 1y-1

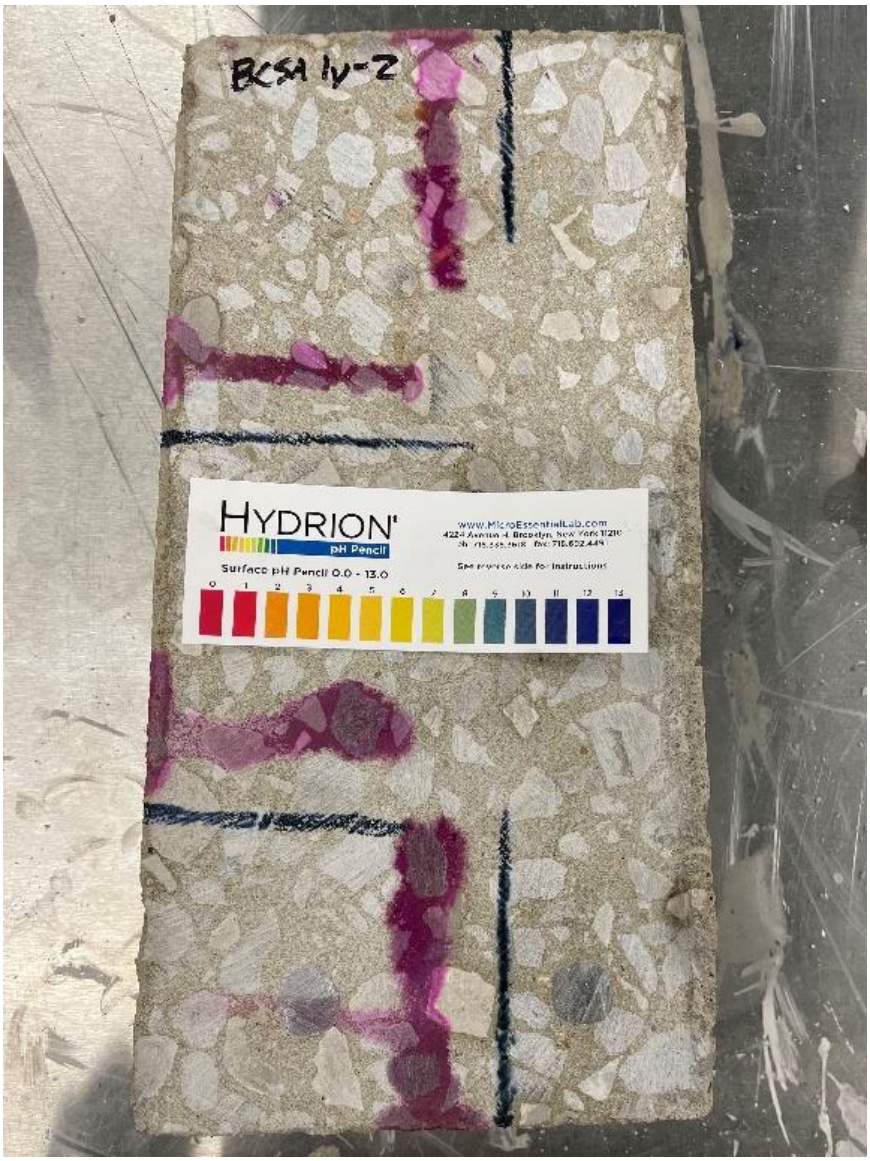

Figure 18. Carbonation test for BCSA 1y-2

4.3 Cracking in Beam Tests

For each beam, a crack diagram was drawn to give a visual representation of the state of the beam after failure. These diagrams can be seen in Figure 19 and are provided together to allow a qualitative look at all the shear tests. Each diagram included the label of the beam and the ultimate load carried by the beam. It was found that all beams failed in shear. PC 1y-1 and PC 1y-2 had different crack patterns than the rest of the beams tested in the study. For PC 1y-1 a

difference in procedure led to inconsistent cracking. Initially, two brackets were screwed into the side of the beams for the end of the LVDT to rest on. It was found that these holes in the beams led to a weak spot that the cracks would propagate through. This can be clearly seen in PC 1y-1 in Figure 19. A flexural crack formed below the point load, an area where the maximum moment would occur, and propagated up through the aforementioned hole to the location where the load was applied. Another crack propagated out of the bracket hole and ran along the longitudinal reinforcement. Ultimately, a shear crack formed, and the beam failed in shear with the concrete crushing at the top. Figure 20 is provided to compare the crack diagram of BCSA 1y-2 with the actual cracked beam.

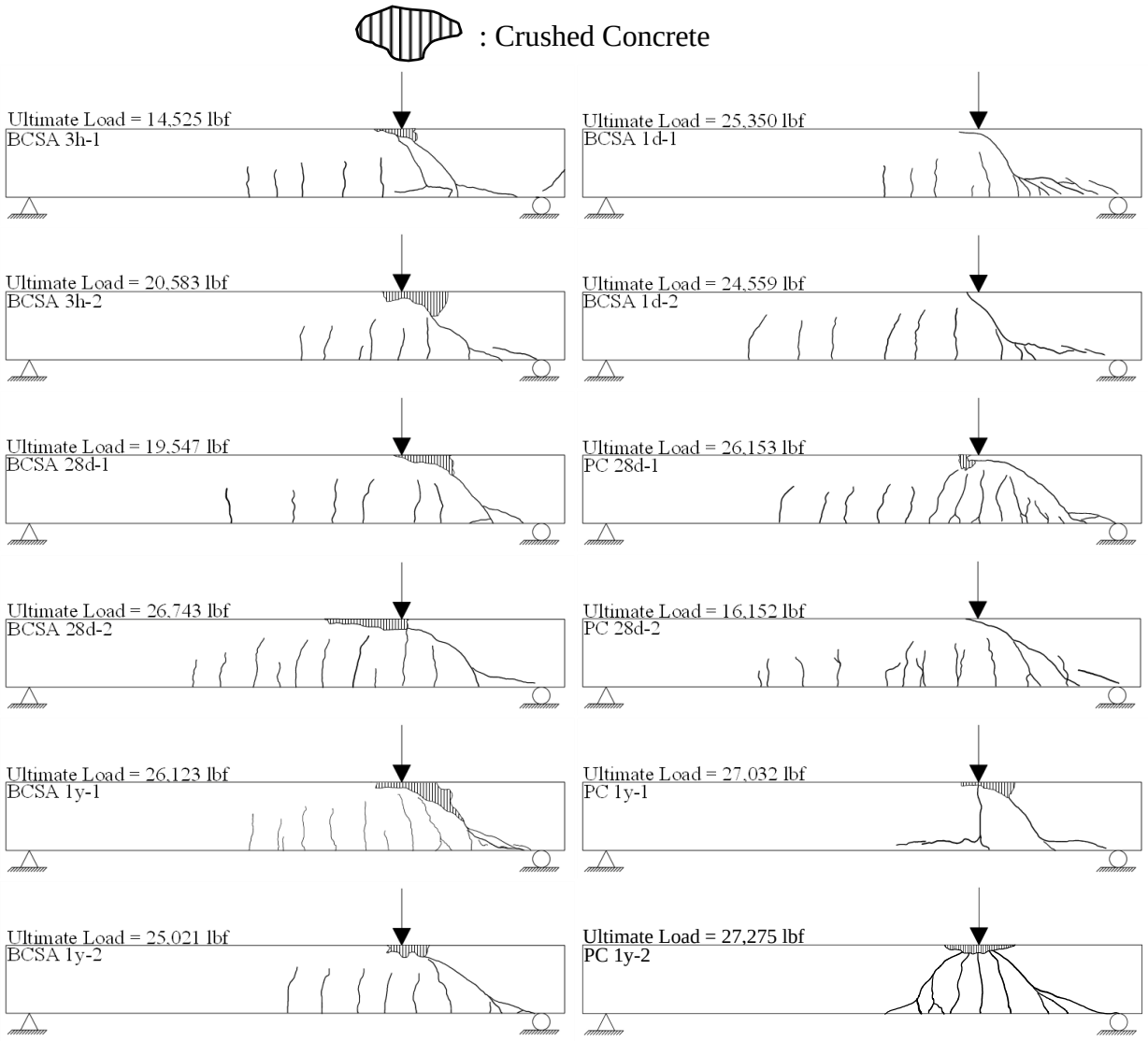

Figure 19. Beam shear test crack diagrams

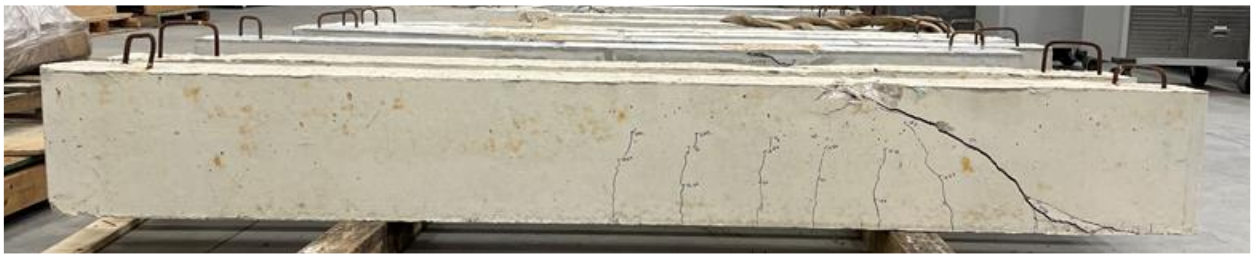

Figure 20. Picture of actual BCSA 1y-2

4.4 Long term compressive strength results

The twelve cores were tested per ASTM C39 and the measured strengths were adjusted per ASTM C42 [1], [34]. The compressive strength for each core and the average of the PC cores and BCSA cores are shown in Table 9. The PC cores had a maximum compressive strength, f'_c, of 12,900 psi, a minimum of 10,850 psi, and an average of 12,250 psi. The BCSA cores had a maximum compressive strength of 9,860 psi, a minimum of 7,810 psi, and an average of 9,160 psi. This test was not to directly compare the strengths of the PC and BCSA cores together, but to get a picture of their respective change in strength over time compared to the companion cylinders cast when the beam was made.

Table 9. Long term compressive strength cylinder break data

Sample	f_c, psi	Average, psi
PC 1y-1 1	12370	12250
PC 1y-1 2	12900	
PC 1y-1 3	12480	
PC 1y-2 1	10850	
PC 1y-2 2	12180	
PC 1y-2 3	12690	
BCSA 1y-1 1	9560	9160
BCSA 1y-1 2	9860	
BCSA 1y-1 3	9600	
BCSA 1y-2 1	9430	
BCSA 1y-2 2	8740	
BCSA 1y-2 3	7810	

5. Discussion of results

5.1 Discussion of shear testing results

Figure 21, seen below, allows for a qualitative look at the variability of the shear test load versus deflection behavior. The consistency of the tests was satisfactory and the variability of

shear strengths on select test ages is attributed to the intrinsic variability of shear in concrete due to the multiple mechanisms at play [23].

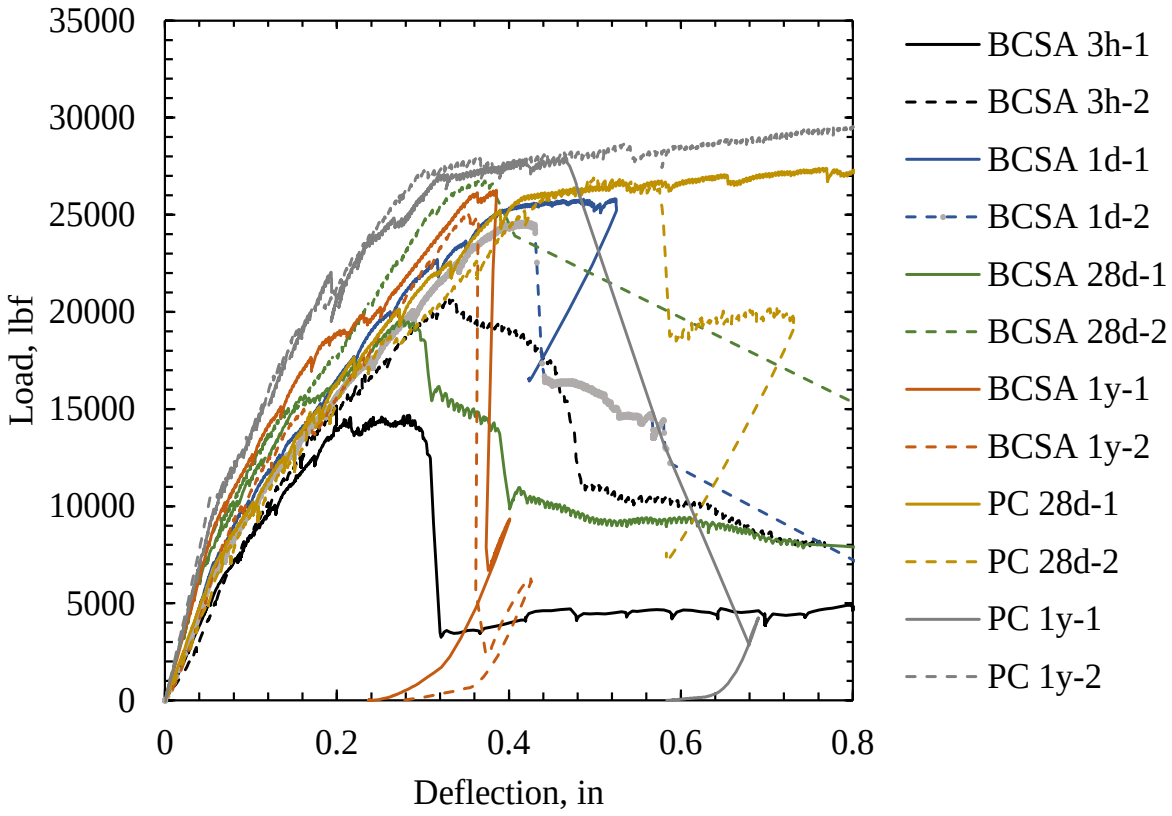

Figure 21. Combined load-deflection plot

The results from the beam shear tests were compared to ACI-318-14/19 [7], Eurocode 2 [9], AASHTO LRFD 2017 [8], and SMCFT [10]. These comparisons can be found in Figure 22. In Figure 22, the error bars for the experimental (Exp) values are the averages of the two beams tested in each sample set. The error bars show the minimum and maximum in the average. It can be seen that the SMCFT provided the closest estimation of the experimental ultimate shear for all beams tested. For all of the test beams except PC 28-day where the SMCFT resulted in an un-conservative predicted strength, the code predicted unfactored shear strengths were lower than the experimental ultimate shear. This aligns with the data shown in Table 10, the codified shear

capacity equations, which are tailored for PC concrete, were more conservative in predicting the capacity of the BCSA cement concrete beams.

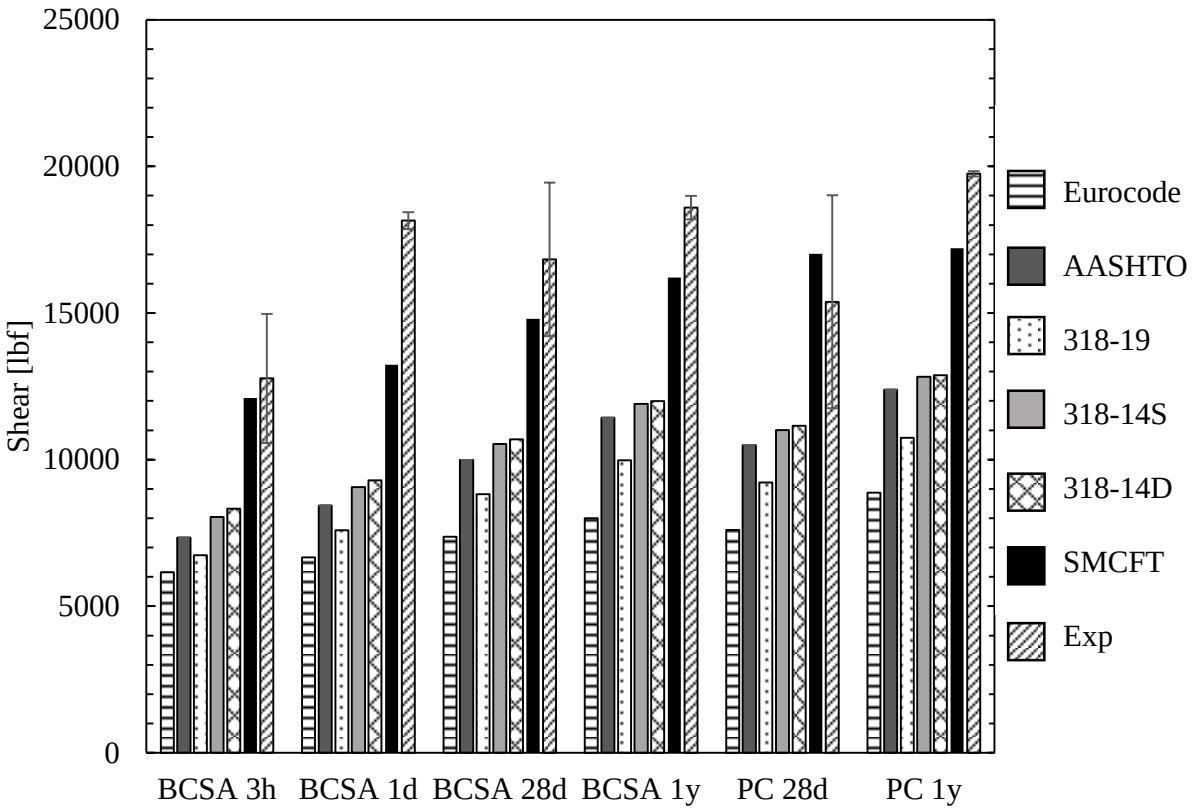

Figure 22. Code nominal shear capacities and ultimate experimental shear

Error bars are plotted over Figure 22 to display the actual ultimate shear of the first and second beam in their respective ages. BCSA 1d, BCSA 1y, and PC 1y had very little difference while BCSA 3h, BCSA 28d, and PC 28d had variable ultimate shears.

Normalized shear strengths are shown in Table 10 to better compare between samples with varying compressive strength. The experimental shear strength, V_{Exp}, was normalized by dividing by $\sqrt{f_c'}b_w d$. An average was taken of the normalized shear strengths of the two replicate specimens tested at each beam age. The BCSA cement concrete beams had a higher ratio of shear strength to the square root of concrete compressive strength compared to the PC

concrete beams. Since "b_w" and "d" were constant for all of the tested beams, the differences in shear strength could be attributed to a larger tension or shear capacity in the BCSA cement for a given compressive strength. It is possible that early age shrinkage in the PC beams led to microcracking that could limit the tension strength and lead to less resistance to shear cracking compared to the BCSA cement which shrinks relatively less.

Table 10. Shear strength normalization

Beam ID	f'$_c$, psi	V_{Exp}, lbf	$\frac{V_{Exp}}{\sqrt{f_c'}b_w d}$	Average $\frac{V_{Exp}}{\sqrt{f_c'}b_w d}$
BCSA 3h-1	3930	10560	2.63	3.18
BCSA 3h-2		14970	3.72	
BCSA 1d-1	4990	18440	4.07	4.01
BCSA 1d-2		17860	3.94	
BCSA 28d-1	6740	14220	2.70	3.20
BCSA 28d-2		19450	3.69	
BCSA 1y-1	8610	19000	3.19	3.13
BCSA 1y-2		18200	3.06	
PC 28d-1	7370	19020	3.00	2.42
PC 28d-2		11750	1.85	
PC 1y-1	11750	19660	2.83	2.84
PC 1y-2		19840	2.85	

A ratio was then taken of the average experimental shear of each set of beams and the predicted shear strengths from the equations in Figure 15, this is defined as the Strength Ratio (SR). These ratios can be seen in Table 11 and graphically in Figure 23. If the SR is a value of 1.0 then the predicted shear equaled the experimental shear. A number above 1.0 means that the prediction was conservative, and below 1.0 means the prediction was unconservative.

Table 11. Strength ratios, Experimental/Predicted

Beam	$V_{exp}/V_{318\text{-}14S}$	$V_{exp}/V_{318\text{-}14D}$	$V_{exp}/V_{318\text{-}19}$	V_{exp}/V_{AASHTO}	V_{exp}/V_{EC2}	V_{exp}/V_{SMCFT}
BCSA 3h	1.588	1.533	1.896	1.741	2.073	1.055
BCSA 1d	2.003	1.952	2.391	2.152	2.721	1.371
BCSA 28d	1.599	1.574	1.908	1.685	2.283	1.137
BCSA 1y	1.563	1.550	1.865	1.628	2.324	1.146
PC 28d	1.397	1.380	1.668	1.466	2.025	0.904
PC 1y	1.540	1.534	1.838	1.595	2.225	1.148

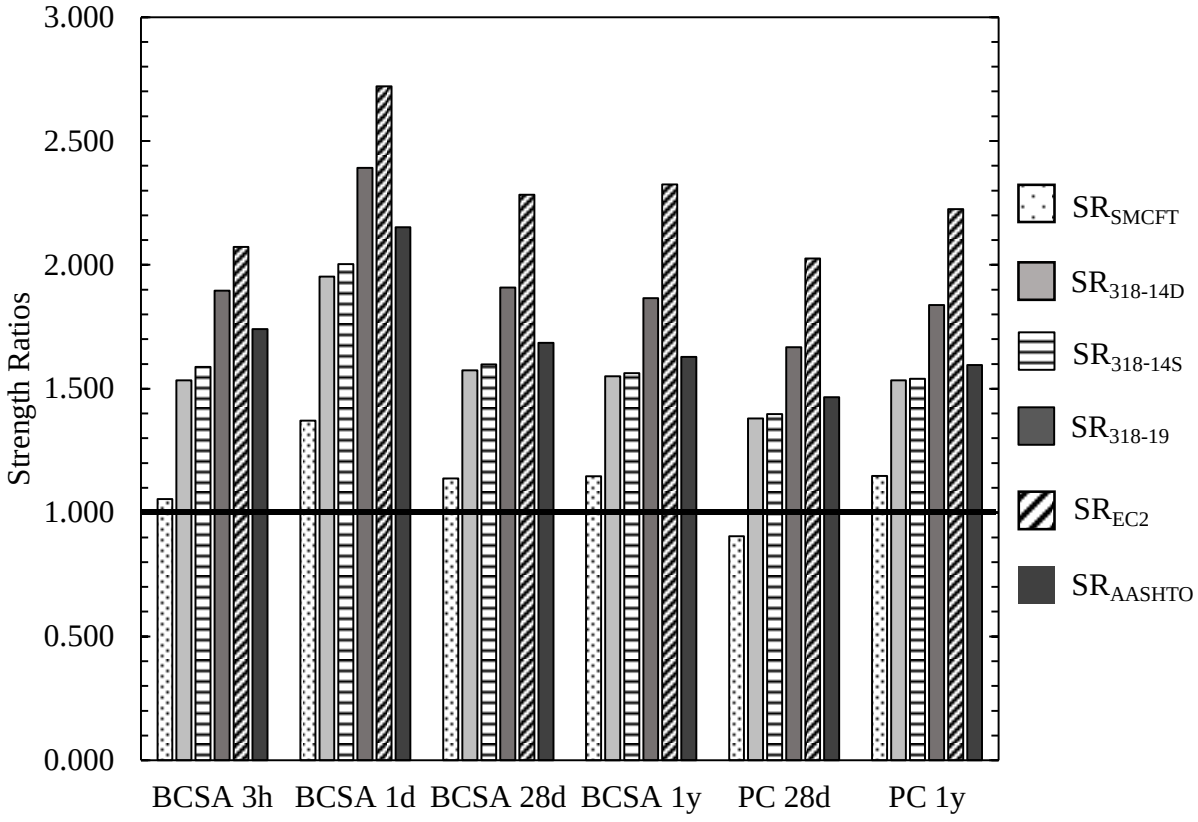

Figure 23. Ratio of experimental shear strength of beams to various shear strength equations

The average strength ratios of the 28 day and 1-year beams, found in Table 12, show that the code estimated shear capacity, on average, was more conservative for the tested BCSA

beams than for the tested PC beams. This could be due to increased tensile strength of BCSA cement concrete. It is known that BCSA cement concrete shrinks less than PC concrete [15], and this could lead to less microcracking in BCSA possibly increasing the tensile strength. More research should be performed in this area to ensure complete understanding of BCSA concrete beam behavior.

Table 12. Average strength ratios for 28-day and 1-year BCSA and PC beams

Beam	$V_{exp}/V_{318\text{-}14S}$	$V_{exp}/V_{318\text{-}14D}$	$V_{exp}/V_{318\text{-}19}$	V_{exp}/V_{AASHTO}	V_{exp}/V_{EC2}	V_{exp}/V_{SMCFT}
BCSA	1.581	1.562	1.887	1.657	2.304	1.142
PC	1.469	1.457	1.753	1.531	2.125	1.026

The angle of the primary shear crack was measured on each beam after it was tested. A line was projected onto the face of the concrete beam, matching the slope of the crack at h/2 where “h” is the height of the beam (theoretical location of maximum shear stress). Following the projection of the line, two measurements were taken. The first measurement was the height of the beam and the second was the horizontal length of the projected line. Using trigonometry, these two distances were used to find the crack angle which is equivalent to the angle of inclination of the compression strut. The comparison of the measured crack angles and the predicted crack angles from the SMCFT can be seen in Figure 24. Based on the measured crack angles, the SMCFT generally provided a good prediction of the angle of inclination of the compression strut and, therefore, the crack angle for both BCSA cement and PC beams. It is important to note that the ACI method makes a simplifying assumption of a 45 degree crack angle.

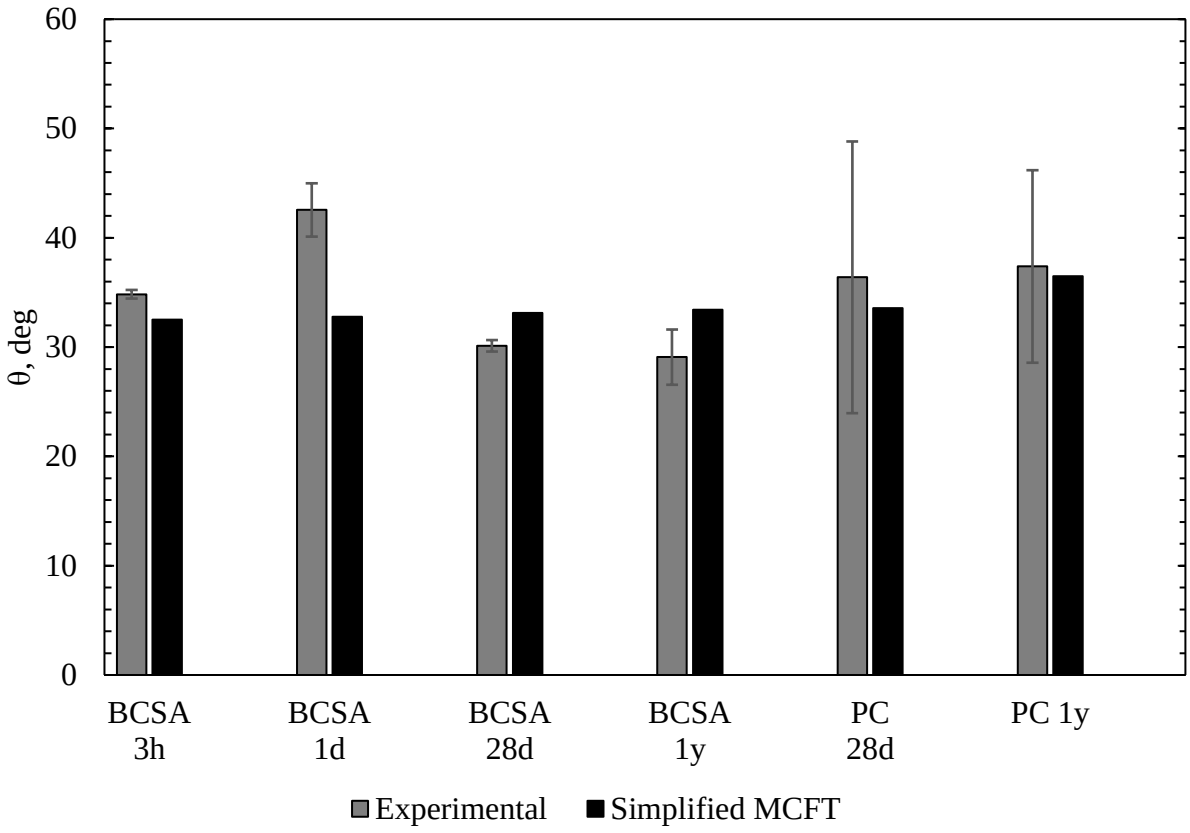

Figure 24. Comparison of Experimental Crack angle and SMCFT

5.2 Discussion of carbonation testing results

It is important for an alternative cement to have limited carbonation so that it can be confidently used in structural applications over long periods of time. The pH testing of BCSA 1y-1, BCSA 1y-2, PC 1y-1, and PC 1y-2 did not indicate a pH below 9, as seen in Figure 15. Furthermore, upon visual inspection of all of the one year beam cross sections, there was no corrosion of the longitudinal reinforcement. Therefore, it is concluded that no carbonation had occurred in any of the one-year beams, at the test locations, over the course of the study.

These results are in contrast to those found by Moffat et al. [29]. Moffat found that the BCSA (called CSA in the paper) samples carbonated at a rate much faster than the control PC

samples. Using the Tuutti model [37], which states that the carbonation rate is proportional to the square root of time, Moffat found a "k" of 7.8mm/yr for the 7 day specimens [29]. In the equation below. "x" is the carbonation depth, "k" the carbonation rate in mm/year, and "t" is time in years [37].

$$x = k\sqrt{t}$$ Tuutti et al. [37]

Given BCSA 1y-1 and BCSA 1y-2 were tested at 466 days or 1.277 years, using Moffat et al. k = 7.8mm/yr., a carbonation depth of 8.81 mm or 0.347 in. would be expected. The difference may be due to the variation in types of BCSA cement that is commercially available and different mix designs.

Another study by Moffatt [38], determined that after one year, in a severe marine environment, the BCSA cement concrete beams had more deterioration, carbonation, and chloride penetration than the control PC concrete beams. This is in contrast to findings by Glasser et al. [39]. Glasser et al. [39] examined a decade old BCSA cement concrete pipe that had been submerged in sea water twice daily due to tides. Upon examination of the pipe, they found that no corrosion or deterioration had occurred in the reinforcing mesh even though there was only 7-8 mm of clear cover [39].

5.3 Discussion of long term compressive strength results

It has been hypothesized that an ettringite based binder such as BCSA will display a reduction in compressive strength over time due to the effects of carbonation [29]. As discussed earlier, past studies such as Moffat et al. [29, 40] found that as ettringite based binders carbonate their porosity increases which results in a loss of strength.

The average compressive strengths from Table 9 were compared with the respective past data from the cylinders cast with the beams. This comparison can be found in Table 13. The average compressive strength in the BCSA cement concrete and PC concrete both continued to increase after one year.

Table 13. Average compressive strength of 1 year mixtures

Age	PC 1y	BCSA 1y
	f'_c, psi	f'_c, psi
3 hours	-	3770
1 day	-	4860
28 days	10140	6600
365 days	11750	8610
471 days	-	9160*
491 days	12250*	-

Note: *indicates average compressive strength obtained from 1-year beam cores

The average compressive strengths over time were plotted in Figure 25 for PC 1y and BCSA 1y. Error bars, at each age, show the minimum compressive strength and maximum compressive strength. In Figure 25, the PC maximum, average, and minimum strengths continue to increase with age. The maximum, average, and minimum strengths of the BCSA 1y mixture were also found to continue to increase after one year as shown in Figure 25.

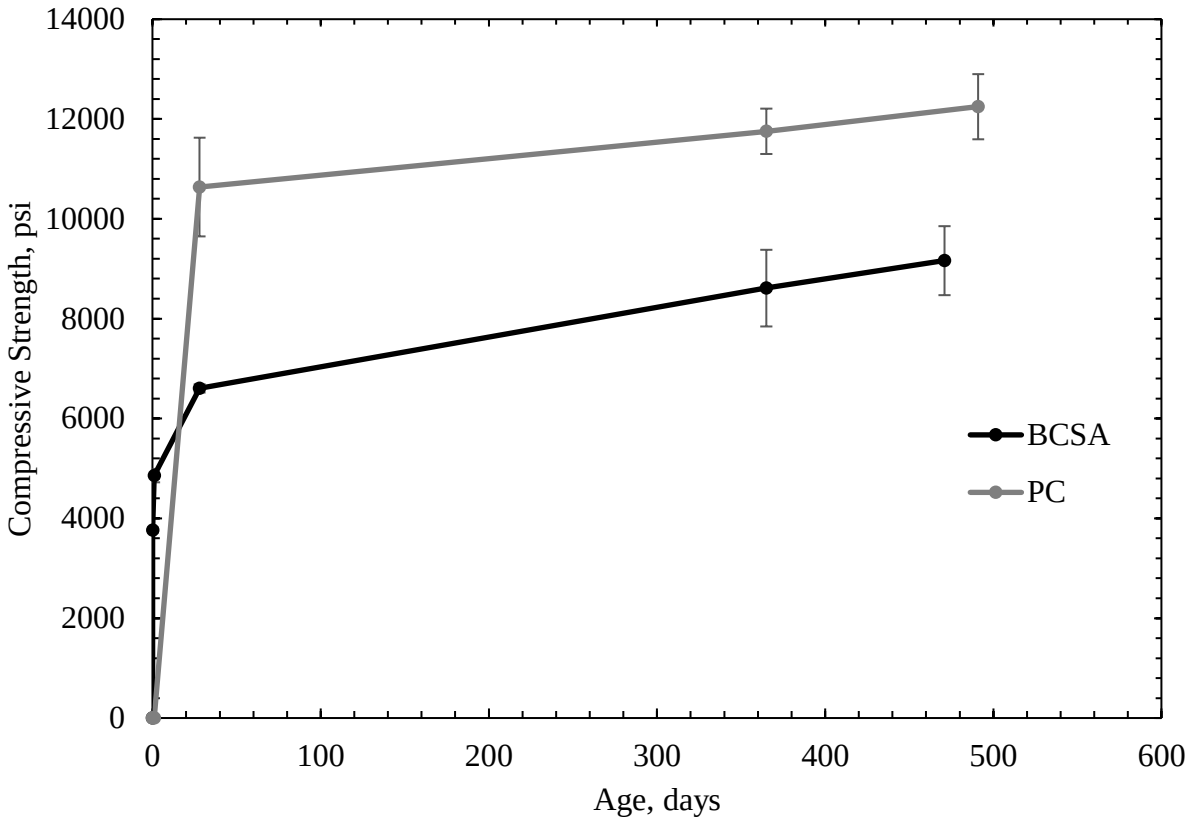

Figure 25. Long-term compression strengths

The increase in compressive strength over time supports the lack of carbonation in the BCSA cement concrete. If significant carbonation had actually occurred and was not measured, we would expect to have a decrease in strength which was not found. If minimal carbonation had occurred and had not been detected, then it likely would not affect the compressive strength of the cores since it would have been in the region of the cylinders that was ground off.

6. Conclusions

This study was performed in order to investigate the shear strength of concrete beams made with BCSA cement with no transverse reinforcement, the carbonation depth of concrete beams made with BCSA cement, and the long term compressive strength of BCSA cement

concrete. An analysis of the data acquired during the duration of the study resulted in the following conclusions:

- BCSA cement concrete beams experience rapid shear strength gains at early ages.
- The shear strength of BCSA cement concrete beams without shear reinforcement was similar to that of PC concrete beams.
- All code equations considered in this study predicted the shear strength of the tested BCSA cement concrete beams more conservatively than the actual shear strength of the tested PC concrete beams.
- The ratio of shear strength of the BCSA cement concrete beams to $\sqrt{f_c'}b_w d$ is greater than that for the PC concrete beams.
- The Simplified Modified Compression Field Theory accurately predicted the shear capacity of the tested BCSA cement concrete beams.
- The ACI code allowable shear strength for reinforced concrete beams with no transverse shear reinforcement is conservative.
- A pH below 9 was not detected in BCSA cement concrete or PC concrete samples.
- The pH of the tested BCSA cement concrete was determined to be 11-12, lower than the PC concrete at 12-13. This determination is subjective and came from the color of the pH indicator.
- Compressive strength gains in the tested BCSA cement concrete continue after 1 year, similar to the tested PC concrete.

Future research on this topic is needed to verify the findings of this study. In addition to replicating the study, additional work needs to be performed. Investigation on the shear behavior of BCSA cement concrete beams with varying sizes needs to be performed. This will allow the

accuracy of the size-effect factor (λs), detailed in ACI 318-19, to be evaluated when applied to BCSA cement concrete beams. Future research should also include investigations in the shear behavior of BCSA cement concrete beams with transverse reinforcement. Further investigation on carbonation of BCSA cement concrete is essential for its practical application in structures. There also needs to be extensive investigation on the mechanism of carbonation in BCSA cement concrete in actual service conditions since the composition of the cement matrix varies greatly from PC concrete.

7. Bibliography

[1] ASTM Standard C42, “Standard Test Method for Obtaining and Testing Drilled Cores and Sawed Beams of Concrete 1”, doi: 10.1520/C0042_C0042M-20.

[2] R. J. Becker, T. C. Holland, and F. S. Malits, “Structural Concrete Using Alternative Cements,” Jun. 2019. [Online]. Available: www.concreteinternational.com|

[3] I. Aguilar Rosero, “Effect of Citric Acid on Slump, Compressive Strength, and Setting Time of Belitic Calcium Sulfoaluminate Concrete,” Fayetteville, Dec. 2020.

[4] L. E. Burris and K. E. Kurtis, “Influence of set retarding admixtures on calcium sulfoaluminate cement hydration and property development,” *Cement and Concrete Research*, vol. 104, pp. 105–113, Feb. 2018, doi: 10.1016/j.cemconres.2017.11.005.

[5] E. O. Soriano, “The Influence of Citric Acid on Setting Time and Temperature Behavior Of Calcium Sulfoaluminate-Belite Cement,” Fayetteville, AR, 2019.

[6] C. W. Chesnut, “Understanding Workability in Belitic Calcium Sulfoaluminate Understanding Workability in Belitic Calcium Sulfoaluminate Concrete Mixtures Concrete Mixtures,” Fayetteville, AR, May 2020. [Online]. Available: https://scholarworks.uark.edu/cveguht

[7] American Concrete Institute, *318-19 Building Code Requirements for Structural Concrete and Commentary*. Farmington Hills, MI: American Concrete Institute, 2019. doi: 10.14359/51716937.

[8] American Association of State Highway and Transportation Officials, “AASHTO LRFD Bridge Design Specifications,” Washington, D.C., 2017.

[9] CEN Technical Committee 250, “EN 1992-1-1: Eurocode 2: Design of concrete structures - Part 1-1: General rules and rules for buildings,” 2004.

[10] E. C. Bentz, F. J. Vecchio, and M. P. Collins, “Simplified Modified Compression Field Theory for Calculating Shear Strength of Reinforced Concrete Elements,” *ACI Structural Journal*, no. July-August, pp. 614–624, 2006.

[11] ACI Committee 318, “Building Code Requirements for Structural Concrete (ACI 318-14) Commentary on Building Code Requirements for Structural Concrete (ACI 318R-14) An ACI Standard and Report from IHS,” Farmington Hills, MI, 2014.

[12] E. P. Bescher, “Calcium Sulfoaluminate-Belite Concrete: Structure, Properties, Practice,” Los Angeles, CA.

[13] B. W. A. Ost, B. Schiefelbein, and J. M. Summerfield, “Very high early strength cement,” US3860433A, Jan. 14, 1975

[14] E. P. Bescher, J. Kim, C. Ramseyer, and J. K. Vallens, “LOW CARBON FOOTPRINT PAVEMENT: HISTORY OF USE, PERFORMANCE AND NEW OPPORTUNITIES FOR BELITIC CALCIUM SULFOALUMINATE,” Jun. 2018.

[15] T. M. Bowser, C. D. Murray, and R. W. Floyd, “Bond behavior of 0.6 in. (15.2 mm) prestressing strand in belitic calcium sulfoaluminate (BCSA) cement concrete,” *ACI Structural Journal*, vol. 117, no. 1, pp. 43–52, 2020, doi: 10.14359/51720196.

[16] J. Kaufmann and F. Winnefeld, “Seasonal heat storage in calcium sulfoaluminate based hardened cement pastes – experiences with different prototypes,” *Journal of Energy Storage*, vol. 25, Oct. 2019, doi: 10.1016/j.est.2019.100850.

[17] R. Maddalena, J. J. Roberts, and A. Hamilton, “Can Portland cement be replaced by low-carbon alternative materials? A study on the thermal properties and carbon emissions of innovative cements,” *Journal of Cleaner Production*, vol. 186, pp. 933–942, Jun. 2018, doi: 10.1016/j.jclepro.2018.02.138.

[18] A. Telesca, T. Matschei, and M. Marroccoli, “Study of eco-friendly belite-calcium sulfoaluminate cements obtained from special wastes,” *Applied Sciences (Switzerland)*, vol. 10, no. 23, pp. 1–14, Dec. 2020, doi: 10.3390/app10238650.

[19] R. J. Thomas, M. Maguire, A. D. Sorensen, and I. Quezada, “Calcium Sulfoaluminate Cement Benefits and applications.” [Online]. Available: www.concreteinternational.com|Ci|APRIL201865

[20] E. Lee Bray, “Bauxite and Alumina 2017,” Reston, VA, 2017.

[21] N. Markosian, R. Tawadrous, M. Mastali, R. J. Thomas, and M. Maguire, “Performance evaluation of a prestressed belitic calcium sulfoaluminate cement (Bcsa) concrete bridge girder,” *Sustainability (Switzerland)*, vol. 13, no. 14, Jul. 2021, doi: 10.3390/su13147875.

[22] G. W. Cook and C. D. Murray, “Behavior of reinforced concrete made with belitic calcium sulfoaluminate cement at early ages,” *ACI Materials Journal*, vol. 117, no. 1, pp. 167–174, 2020, doi: 10.14359/51719074.

[23] N. M. Hawkins, D. A. Kuchma, R. F. Mast, M. L. Marsh, and K.-H. Reineck, “NCHRP Web-Only Document 78 (Project 12-61): Contractor’s Final Report-Appendixes Simplified Shear Design of Structural Concrete Members Appendixes,” Washington, DC, Jul. 2005. [Online]. Available: www.TRB.org

[24] D. A. Kuchma, S. Wei, D. H. Sanders, A. Belarbi, and L. C. Novak, “Development of the one-way shear design provisions of ACI 318-19 for reinforced concrete,” *ACI Structural Journal*, vol. 116, no. 4, pp. 285–295, 2019, doi: 10.14359/51716739.

[25] A. T. Moczko, N. J. Carino, and C. G. Petersen, “CAPO-TEST to estimate concrete strength in bridges,” *ACI Materials Journal*, vol. 113, no. 6, pp. 827–836, Nov. 2016, doi: 10.14359/51689242.

[26] A. T. Moczko, N. J. Carino, and C. G. Petersen, “CAPO-TEST to estimate concrete strength in bridges,” *ACI Materials Journal*, vol. 113, no. 6, pp. 827–836, Nov. 2016, doi: 10.14359/51689242.

[27] Y. Li, W. Guo, and H. Li, “Method to Calculate Cement Content in Hardened Concrete Based on Theory of Carbonization,” *ACI Materials Journal*, vol. 114, no. 2, Apr. 2017, doi: 10.14359/51689491.

[28] Y. Sumra, S. Payam, and I. Zainah, “The pH of Cement-based Materials: A Review,” *Journal Wuhan University of Technology, Materials Science Edition*, vol. 35, no. 5. Wuhan Ligong Daxue, pp. 908–924, Oct. 01, 2020. doi: 10.1007/s11595-020-2337-y.

[29] E. G. Moffatt and M. D. A. Thomas, “Effect of carbonation on the durability and mechanical performance of ettringite-based binders,” *ACI Materials Journal*, vol. 116, no.1, pp. 95–102, 2019, doi: 10.14359/51710965.

[30] ASTM, “Designation: C566-19 Standard Test Method for Total Evaporable Moisture Content of Aggregate by Drying 1.” doi: 10.1520/C0566-19.

[31] ASTM Standard C128, “Standard Test Method for Relative Density (Specific Gravity) and Absorption of Fine Aggregate 1”, doi: 10.1520/C0128-15.

[32] ASTM Standard C127, “Standard Test Method for Relative Density (Specific Gravity) and Absorption of Coarse Aggregate 1”, doi: 10.1520/C0127-15.

[33] ASTM, “Designation: C143/C143M − 15a Standard Test Method for Slump of Hydraulic-Cement Concrete 1.” doi: 10.1520/C0143_C0143M-15A.

[34] ASTM Standard C39, “Standard Test Method for Compressive Strength of Cylindrical Concrete Specimens 1”, doi: 10.1520/C0039_C0039M-21.

[35] A. T. Omar and A. A. A. Hassan, “Shear behavior of lightweight self-consolidating concrete beams containing coarse and fine lightweight aggregates,” *ACI Structural Journal*, vol. 118, no. 3, pp. 175–186, May 2021, doi: 10.14359/51729361.

[36] J. Lima, L. Reis, and D. Oliveira, “A Model for Shear Resistance of Reinforced Concrete Beams,” *ACI Structural Journal*, vol. 118, no. 5, Sep. 2021, doi: 10.14359/51732863.

[37] K. Tuutti, “Corrosion of steel in concrete,” *Swedish Cement and Concrete Research Institute*. Stockholm, 1982.

[38] E. G. Moffatt and M. D. A. Thomas, “Performance of rapid-repair concrete in an aggressive marine environment,” *Construction and Building Materials*, vol. 132, pp. 478–486, Feb. 2017, doi: 10.1016/j.conbuildmat.2016.12.004.

[39] F. P. Glasser and L. Zhang, “High-performance cement matrices based on calcium sulfoaluminate-belite compositions,” *Cement and Concrete Research*, pp. 1881–1886, Aug. 2001.

[40] E. G. Moffatt and M. D. A. Thomas, “Durability of rapid-strength concrete produced with ettringite-based binders,” *ACI Materials Journal*, vol. 115, no. 1, pp. 105–115, Jan. 2018, doi: 10.14359/51701006.

8. Appendix

Please see supplementary files.